AN ABSTRACT OF THE THESIS OF

JANE ANN COPELAND for the degree of MASTER OF SCIENCE

in Civil Engineering presented on June 7, 1979

Title: FABRICS IN SUBDRAINS: MECHANISMS OF FILTRATION AND THE MEASUREMENT OF PERMEABILITY

Redacted for Privacy

Abstract approved: ______________

The roles of fabrics in subdrains are identified for normal groundwater flow conditions to determine hydraulic and pore characteristics necessary for design considerations. Two conditions are discussed: (1) the fabric in direct contact with the soil to provide mechanical support, and (2) the fabric as a filter to remove soil particles in suspension in water. If direct contact is maintained between the soil and fabric, control of the hydraulic gradient and/or pore size will prevent soil migration and fabric plugging by soil particles. If the fabric is a filter in the sense that it removes soil particles suspended in water, the fabric will plug. For this case a method of controlling piping of suspended soil particles by relating a soil grain size to the coefficient of fabric permeability is proposed. Relationships between a soil grain size, the soil Reynolds number, and the soil cake porosity are suggested as means of evaluating the effect of fabric plugging and soil cake formation. An experimental design is proposed to evaluate the applicability of the

proposed equations for the critical hydraulic gradient and the control of plugging and piping.

Air permeability and falling head water permeability tests were performed. The falling head test provided for water and fabric deairing. Turbulence was found to exist when testing one layer of fabric but laminar flow was indicated when testing multiple layers. Comparison between air and water permeability test results indicates that either method can predict fabric permeability with satisfactory accuracy.

Fabrics in Subdrains: Mechanisms of Filtration and the Measurement of Permeability

by

Jane Ann Copeland

A THESIS

submitted to

Oregon State University

in partial fulfillment of
the requirements for the
degree of

Master of Science

Completed June 7, 1979

Commencement June 1980

APPROVED:

Redacted for Privacy

Professor of Civil Engineering
in charge of major

Redacted for Privacy

Head of Department of Civil Engineering

Redacted for Privacy

Dean of Graduate School

Date thesis is presented June 7, 1979

Typed by Deanna L. Cramer for Jane Ann Copeland

TABLE OF CONTENTS

Table of Contents -- continued

LIST OF FIGURES

LIST OF TABLES

NOTATION

Term	Description	Dimensions
A	Cross sectional area	L^2
a	Area of cylinder	L^2
A_1	Filter constant.	$L^{-1}T^{-1}$
A_s	Area of fabric fibers.	L^2
A_T	Total fabric area.	L^2
C	Empirical constant	Dimensionless
$\bar{d}$	Mean particle diameter	L
D_{15}	Grain size for which 15% of the material is finer by weight.	L
D_{85}	Grain size for which 85% of the material is finer by weight.	L
d_p	Maximum pore over which bridging may occur . . .	L
D_s	Mean diameter of smaller sized material.	L
E_o	At rest earth pressure	FL^{-2}
F_s	Seepage force.	FL^{-3}
h	Height of seepage from drain base at distance x from drain centerline.	L
h_1	Piezometer reading 1	L
h_2	Piezometer reading 2	L
h_3	Piezometer reading 3	L
h_4	Piezometer reading 4	L
H_{c1}	Height of soil cake between fabric and piezometer 2	L
H_{c2}	Total height of soil cake.	L
h_d	Height of seepage from drain base at distance x_d from drain centerline	L

Term	Description	Dimensions
h_f	Height of seepage from drain base at distance x_f from drain centerline	L
h_f	Height of water at end of test	L
h_i	Height of water at beginning of test	L
h_L	Head loss at interface	L
H_s	Height of soil	L
H_{sa}	Height of unaffected soil.	L
H_{st}	Total height of soil	L
i	Hydraulic gradient	Dimensionless
i_c	Critical hydraulic gradient.	Dimensionless
K	Permeability	L^2
k	Coefficient of permeability.	LT^{-2}
k_a	Coefficient of fabric permeability computed from air permeability results.	LT^{-1}
k_{ap}	Permittivity determined from air permeability. .	T^{-1}
K_c	Kozeny-Carman cake permeability.	L^2
k_c	Coefficient of soil cake permeability.	LT^{-1}
k_{eq}	Equivalent soil-fabric coefficient of permeability	LT^{-1}
k'_{eq}	Unplugged equivalent coefficient of permeability	LT^{-1}
k_f	Coefficient of fabric permeability	LT^{-1}
k_{fp}	Coefficient of plugged fabric permeability . . .	LT^{-1}
K_k	2 to 5, depending on bed structure	Dimensionless
K_o	Coefficient of at rest earth pressure.	Dimensionless
k_p	Permittivity	T^{-1}

Notation -- continued

Term	Description	Dimensions
k_s	Coefficient of soil permeability	LT^{-1}
L	Thickness of fabric.	L
L_{3-4}	Height of soil between piezometers 3 and 4 . . .	L
L_{sf}	Height of soil plus fabric thickness	L
n	Turbulence coefficient	Dimensionless
n_k	Constant exponent.	Dimensionless
n_p	Fabric porosity.	Dimensionless
n_t	Number of timings required	Dimensionless
q	Quantity of flow per unit time	L^3T^{-1}
q_o	Overburden pressure.	FL^{-2}
Re	Reynolds number.	Dimensionless
r_i	Maximum pore radius.	L
r_o	r_i plus fiber diameter	L
S_o	Specific surface	L^{-1}
t	Time	T
v	Flow velocity.	LT^{-1}
W_a	Pressure on soil from overburden above fabric at depth y	FL^{-2}
W_o	Force on fiber from overburden	F
W_p	Passive force on fibers due to aggregate	F
W_{pd}	Distributed pressure on the soil resulting from W_p.	FL^{-2}
W'_s	Effective weight of soil	FL^{-3}
x	Distance from drain centerline to any point. . .	L

Notation -- continued

Term	Description	Dimensions
x_d	Distance from drain centerline to inner edge of fabric surface.	L
x_f	Distance from drain centerline to outer edge of fabric surface.	L
y	Depth below fiber level.	L
z	Depth of overburden.	L
γ	Fabric unit weight	FL^{-3}
$\gamma_{20°C}$	Unit weight of water at 20°C	FL^{-3}
γ_a	Unit weight of overburden.	FL^{-3}
γ_f	Unit weight of fabric solids	FL^{-3}
γ_s'	Effective unit weight of soil.	FL^{-3}
γ_w	Unit weight of water	FL^{-3}
Δh	Head loss.	L
Δhc	Head loss across soil cake	L
Δh_p	Head loss across plugged fabric.	L
Δh_T	Total head loss.	L
ΔP	Pressure drop across fabric.	L
Δp_b	Pressure drop across fabric when bubble appears.	FL^{-2}
δ	Largest particle that will pass a filter	L
ε	Cake porosity.	Dimensionless
θ	Contact angle.	Degrees
μ	Absolute viscosity of air at 70°F	$Ft\ L^{-2}$
$\mu_{20°C}$	Absolute viscosity of water at 20°C.	FL^{-2}
μ_T	Absolute viscosity of water at test temperature.	FTL^{-2}

Notation -- continued

Term	Description	Dimensions
ν	Coefficient of variation	Percent
ν_k	Kinematic viscosity.	L^2T^{-1}
σ	Surface tension.	FL^{-1}

FABRICS IN SUBDRAINS:
MECHANISMS OF FILTRATION AND THE MEASUREMENT OF PERMEABILITY

I. INTRODUCTION

Control of subsurface water is often a problem during and after construction of an engineering project. Drainage must be provided such that excessive water pressures or seepage forces do not develop. Inadequate drainage may result in the instability of a soil mass, with subsequent structural failure.

The need for adequate drainage of highways has become especially apparent in recent years with the increasing number of pavement failures attributed to poor drainage [44]*. Conventional drainage design normally specifies graded aggregate filters such that soil movement into hydraulic structures is prevented. However, due to recent technological advances in the textile industry and the depletion of suitable aggregate sources, fabrics have gained increased acceptance as effective filters in drainage systems. Drainage applications that might incorporate a fabric as a filter medium include trench drains, French drains, wrapped pipes, base course drains, and structural drains such as behind retaining walls and rock buttresses. The replacement of conventional aggregate filters with fabric reduces the amount of aggregate needed, eliminates the need for strict gradation control during filter placement, provides greater ease of construction, and, in most cases, reduces the overall cost of the drain.

---

*Numbers in brackets refer to items in the Bibliography.

Unfortunately, the rapid increase in fabric usage has not been accompanied by the development of suitable design technology. Basically, it is known that the filter fabric must satisfy two requirements in filtration applications. First, the fabric must be sufficiently permeable to allow removal of groundwater without the buildup of excessive water pressures. Second, the fabric must be able to prevent piping or subsurface erosion of the soil mass being drained. Current specifications [38, 39] attempt to satisfy these requirements by specifying a characteristic pore size and/or the fabric permeability. Although most installations built to these specifications have been successful, there is not a sound basis for the acceptance or rejection of these specifications. A general theory of filtration mechanisms necessary for the design of a fabric filter is not available at this time.

Purpose and Scope

The purposes of this investigation are to explain the filtration processes and mechanisms in a soil-fabric-drain system and to investigate measurement of fabric permeability.

The scope of this project is limited to seepage cases which develop as a result of seepage conditions. Surging or pumping conditions which develop as a result of wave or repetitive traffic loads are not covered. Although experimental and theoretical discussions generally apply to all filtration applications, attention is focused on trench drain. The study begins with a review and analysis of the literature pertaining to fabric filter design. Significant fabric properties to minimize particle migration and ensure adequate drainage are next identified. Test development is restricted to measurement of hydraulic and filtration characteristics only. In addition, data are collected from permeability tests only. The influences of biological growth and chemical or mechanical degradation on filtration behavior are not considered.

II. BACKGROUND

Background information is provided in this section in the form of a literature review. Analysis is also included to provide background necessary for later development of filtration mechanisms, tests, and specifications.

Filtration Cases

Four distinct conditions of filtration are identified. Three of these are illustrated in Figure 1. In Case 1, the fabric is in direct contact with the soil. This condition is expected to dominate in most installations.

In Case 2, there is a gap between the fabric and the soil. This condition has been reported by the New York Department of Transportation [29]. This situation may be common, since variations in soil conditions may contribute to irregular trenches caused by boulders, cave-ins, and other factors. Case 2 may be reduced to Case 1 if the fabric is sufficiently flexible to conform to the shape of the cavity during aggregate placement.

In Case 3, a soil-water mixture is filtered by the fabric. As heavy traffic passes and water and soil are ejected at high pressures directly onto the fabric. This process may lead to the development of a void behind the fabric. Alternatively, a soil cake on the fabric may form if the fabric plugs with soil particles. Fabric plugging may develop if one or both of the following occur: (1) soil particles

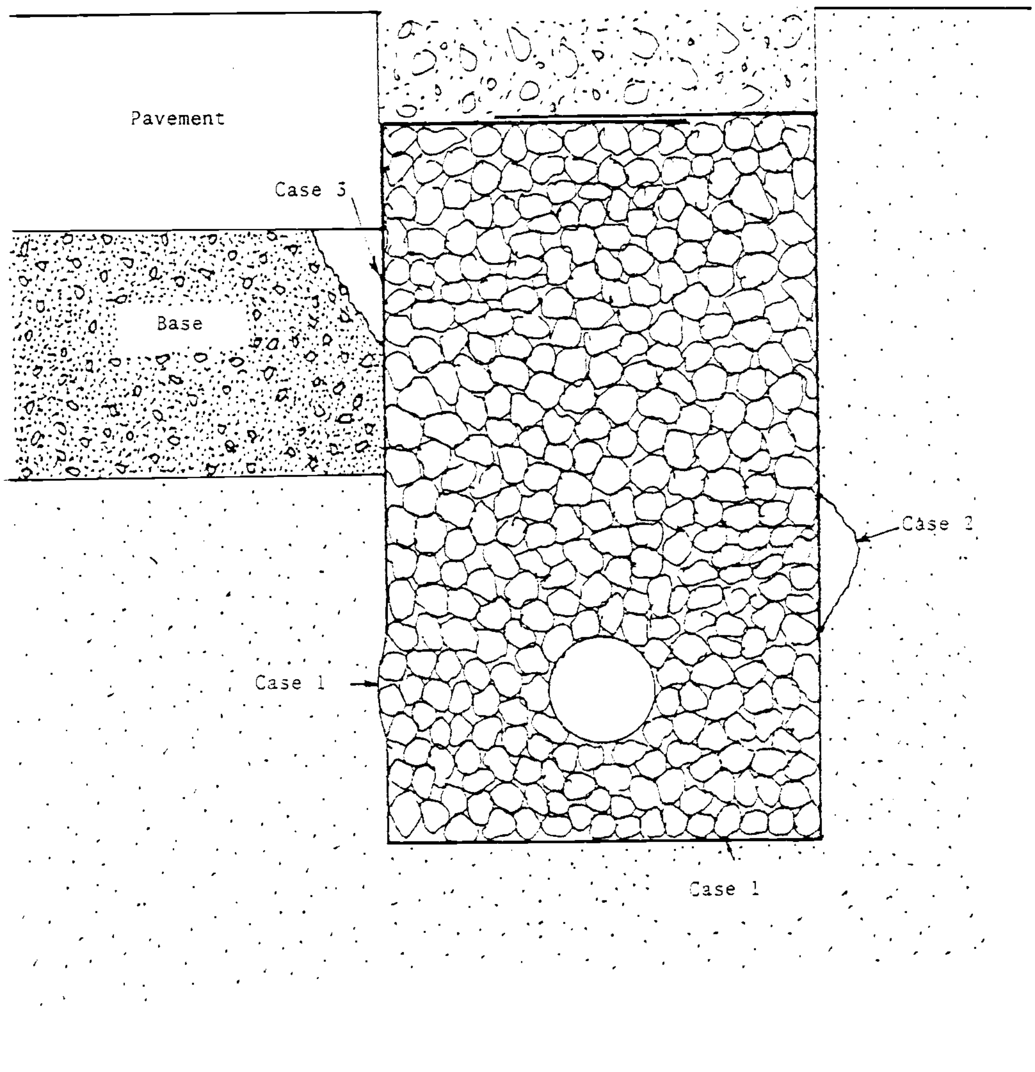

FIGURE 1. Filtration Cases

become trapped in surface fabric pores (i.e. blinding), or (2) soil particles become entrapped within the fabric thickness (i.e. clogging). Figure 2 illustrates both methods of plugging. Fabric plugging may significantly reduce the permeability of the fabric and thereby prevent the removal of water from beneath the pavement and the stability of the base may be reduced. This phenomenon has been reported by the Georgia Department of Transportation [14].

In Case 4, the fabric is exposed to water containing suspended solids. This situation might occur during the construction phase if the trench extends below the groundwater table. Alternatively, rainfall during construction might wash fine particles into the fabric. In a laboratory study, it was found that fabrics become plugged when exposed to dirty ditch water [19].

In terms of soil types, silts and fine sands present the most troublesome cases of particle migration or plugging. Gulati, et al. [17] have noted that saturated uniform porous media with particle diameters from 0.1 mm to 0.25 mm are the most critical for causing sedimentation in subsurface agricultural drains. Permeabilities are high and the velocities required to cause particle motion are low. On the other hand, clay soils are not normally troublesome because of their very low permeabilities and the high gradients that are necessary to achieve the velocity to set the particles in motion. Strong attraction between clay particles minimize particle migration.

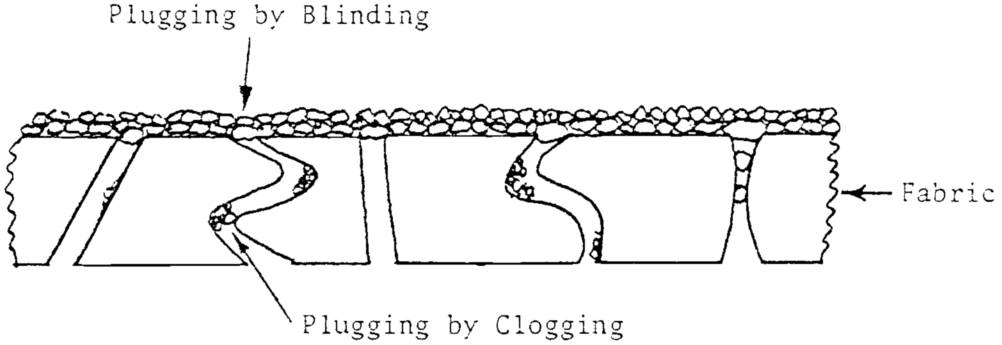

FIGURE 2. Plugging of a Filter Fabric

Fabric Types

The development of filtration mechanisms requires a general understanding of the commonly used fabrics. Fabrics may be divided into two broad groups: (1) woven fabrics and (2) nonwoven fabrics. Both types may be manufactured from one or a combination of the following polymers: (1) polypropylene, (2) polyester, (3) nylon, (4) polyethylene, and (5) polyvinylidene chloride. The first two polymers are most commonly used.

Woven fabrics are characterized by a highly ordered structure in which fibers or yarns are oriented perpendicular to and overlap each other. Woven fabrics may be multifilament, monofilament or slit film. Multifilament fabrics are woven from yarns composed of many filaments. Small pores exist within these yarns. Monofilament fabrics are woven from strands which are single filaments. Pores are relatively uniform, with a much lower degree of tortuosity than those found in nonwoven fabrics. Slit film fabrics are woven from ribbons of thin polypropylene sheets. Slit film woven fabrics are less uniform than the monofilament fabrics. Since the ribbons are not bonded together, they may separate and alter the pore characteristics.

Three types of nonwoven fabrics are widely used in filtration applications. These are: (1) heat bonded fabrics, (2) resin bonded fabrics, and (3) needle punched fabrics. The fabrics differ in the method of joining the randomly oriented filaments. The fiber filaments may be either continuous or staple. Continuous filaments are extruded and drawn in one continuous fiber. Staple filaments are cut to a specified length, which may vary from less than an inch to several inches.

Heat bonded fabrics are formed by subjecting fabric mats to high temperatures and thereby "welding" the fibers together. In resin bonded fabrics, the fibers are cemented together by a resin which coats the fibers. Both resin bonded and heat bonded fabrics are characterized by irregular pore sizes and distributions. Since they are normally relatively thin, there should be a low degree of tortuosity in the pores. Needle punched fabrics consist of fibers that are mechanically interlocked by repeated entry of barbed needles that compact and entangle individual fibers. In addition to possessing irregular pore sizes and distributions, needle punched fabrics are commonly thicker and characterized by pores with a high degree of tortuosity.

Combinations of woven and nonwoven fabrics are available.

Table 1 summarizes the above construction groups.

Fabric Characteristics and Filtration

Several fabric characteristics have been considered to affect fabric performance in filtration applications. These characteristics are identified in the following paragraphs.

Pore Size

The largest pore size controls the maximum size soil particle that can possibly migrate through the fabric. The radius of the maximum pore (r_i) may be obtained as follows, from bubble pressure test results [8, 42]. For r_i in centimeters:

$$r_i = \frac{2 \times 10^{-6}\, \sigma \cos \theta}{\Delta\, p_b} \qquad (1)$$

Table 1. Fabric Construction Groups.

Structure	Filament	Bonding
Woven	Monofilament	Heat Bonded None
	Multifilament	None
	Ribbon Filament	None
Knitted	Multifilament	None
Nonwoven	Staple Filament	Needle Punched Heat Bonded Resin Bonded Combination
	Continuous Filament	Needle Punched Heat Bonded Resin Bonded Combination
Combination and Woven-Nonwoven	All combinations of above	All combinations of above
Special	Other Methods	Other Methods

where: σ = surface tension, dynes/cm

θ = contact angle, degrees

Δp_b = pressure drop across fabric when first bubble appears, kN/m^2.

However, since soil migration will also depend upon the number of large pores, a more appropriate method of fabric characterization might be the pore size distribution. Fabric characterization according to pore size or distribution required for specification purposes will depend upon the filtration mechanism involved.

Fiber Characteristics

Fiber diameter may affect the pore size, as shown in Figure 3. For a unit area, two fabrics may have the same percent open area, but the fabric with larger fibers will have fewer but larger openings, while the fabric with smaller fibers will have more openings that are smaller in size. Piping for Fabric B may be either greater than or equal to piping for Fabric A. That is, the probability of piping depends upon the fabric pore sizes as well as the soil grain sizes. For instance, if the pore sizes in Fabric A were large enough to permit particle migration, piping might be equal for both fabrics. On the other hand, if the soil grains were larger than the pore sizes in Fabric A, but smaller than the pore sizes in Fabric B, piping would be greater for Fabric B. Therefore, it appears that the percent open area alone may not be an accurate means of predicting particle migration.

Fiber diameter may also affect fabric permeability or system permeability when in contact with soil. Both fabrics may have the same

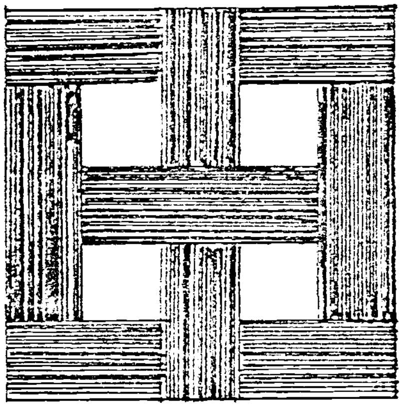

FABRIC A

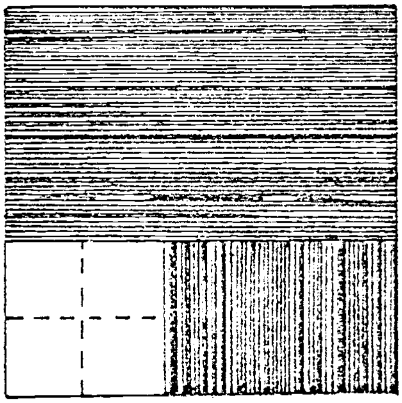

FABRIC B

FIGURE 3. Effect of Fiber Diameter on Pore Size

average permeability in the absence of soil. However, Fabric B may appear less permeable than Fabric A when placed adjacent to identical soils because in the first instance water may have to travel horizontally to reach an opening. In addition, the concentration of flow paths at the pore opening would result in increased gradients in this vicinity. The increased gradients could in turn be accompanied by turbulence and piping. This idealized concept is illustrated in Figure 4. This behavior should be less pronounced if grain sizes are fairly large relative to the fiber diameter, since horizontal flow resistance would be less for large grain sizes, compared to the flow resistance for smaller sizes.

Thickness

Soil particle migration depends on the size of the continuous fabric opening. For thicker fabrics, particularly nonwovens, the continuous openings may be tortuous and possibly reduce the maximum size of migratory particles. As soil particles become entrapped within the fabric structure, the effective area for flow is reduced, and the potential for clogging is increased [35]. Thicker fabrics may be more likely to clog than thinner fabrics, because there is a greater opportunity for soil particles to be trapped since the fabric flow path is longer and hydraulic gradients are smaller.

Rigidity of Structure

For less rigid fabrics, pores may tend to close up under compression. Laboratory tests on fabrics have indicated a reduction in void

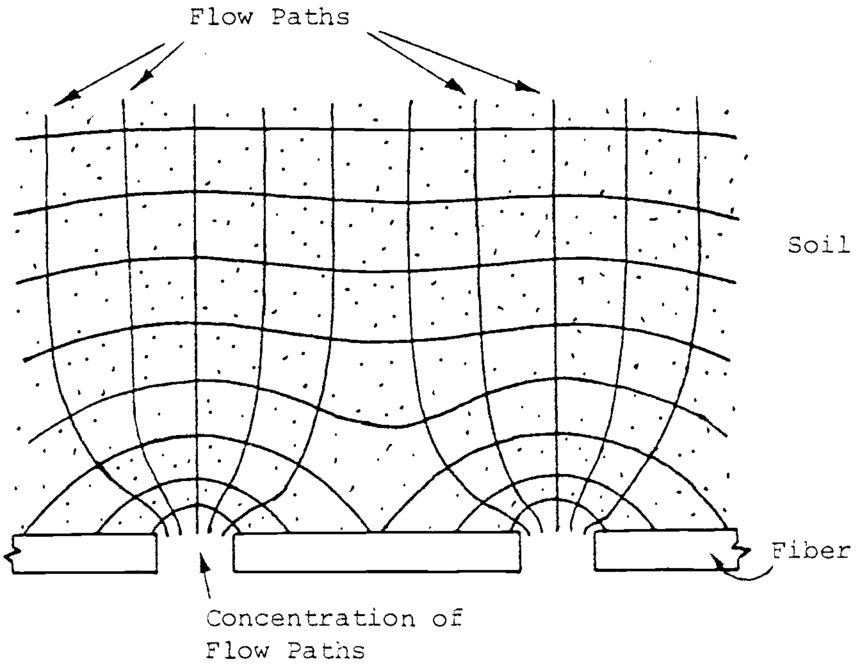

FIGURE 4. Effect of Fiber Diameter on Flow

ratio and permeability when subjected to increased normal stresses [8]. When this happens permeability and the likelihood of piping may decrease. The fabric may be more susceptible to plugging. Alternatively, if the fabric stretches, pore sizes may increase, thereby increasing the fabric permeability and piping potential and decreasing plugging.

Filtration Theories

When selecting a fabric for a drainage installation, it is necessary to understand the mechanisms involved in filtration behavior. In terms of particle migration and clogging potential, the four filtration cases presented earlier reduce to two types of filtration behavior: (1) the soil is in intimate contact with the fabric and the water does not contain suspended solids, or (2) individual soil particles are suspended in flowing water.

By definition, a filter is "any porous substance through which a liquid or gas is passed in order to remove certain constituents" [4]. Extensive research has been conducted in the areas of industrial and chemical filtration to examine the structure and performance of filters [9, 12, 16, 42]. Clearly, in this case, the filter must plug and become less permeable if it is to fulfill its purpose. If fabrics serve as true filters in subdrains, the net result would be detrimental to the overall performance of the drain. That is, the fabric would plug, its permeability would be reduced, and the original purpose of removing subsurface water would be defeated. However, it is known that subdrainage systems such as trench drains that involve fabric in intimate contact with the soil have performed satisfactorily in both the United States and Europe for many years [13, 22, 27, 28, 29, 35]. Therefore, the fabric must not serve as a true filter in this case, since it continues to function without detrimental plugging.

An interpretation of soil-fabric filtration behavior can be explained through studies conducted at Utah State University [6, 43]. Based on experimental results, it was found that when the soil grains are smaller than the fabric opening, arches develop over the openings of the fabric or screen as shown in Figure 5. The filter material functions only as a means of mechanical support, provided that the failure hydraulic gradient of the soil is not exceeded. The support provided by the individual strands of the filter medium is evidenced by the development of the shallow arches between the restraining fabrics. Walker [43] observed that the arch slightly deepened with increases in gradient resulting from flow rate increases. The deepening of the arch was explained as an attempt of the arch to reach an equilibrium by maintaining a constant gradient at the soil-water interface by increasing the surface area of flow. When the arch was no longer able to modify its depth to accommodate further increases in the flow rate, the failure gradient was exceeded, the arch collapsed, and the sample failed by piping.

Utah State University studied filtration behavior in laboratory investigations that tested five different soils, three fabrics, and selected metal screens to determine the interaction of the filter medium with the soils. The soils contained large portions of silt and clay size particles. Figure 6 gives grain size distribution curves for

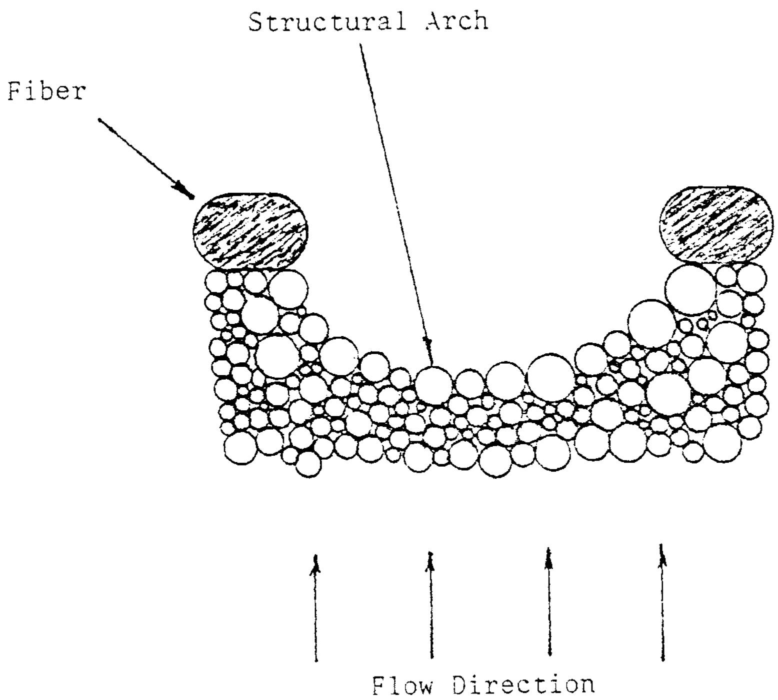

FIGURE 5. Structural Arches in Soil Adjacent to Fabric

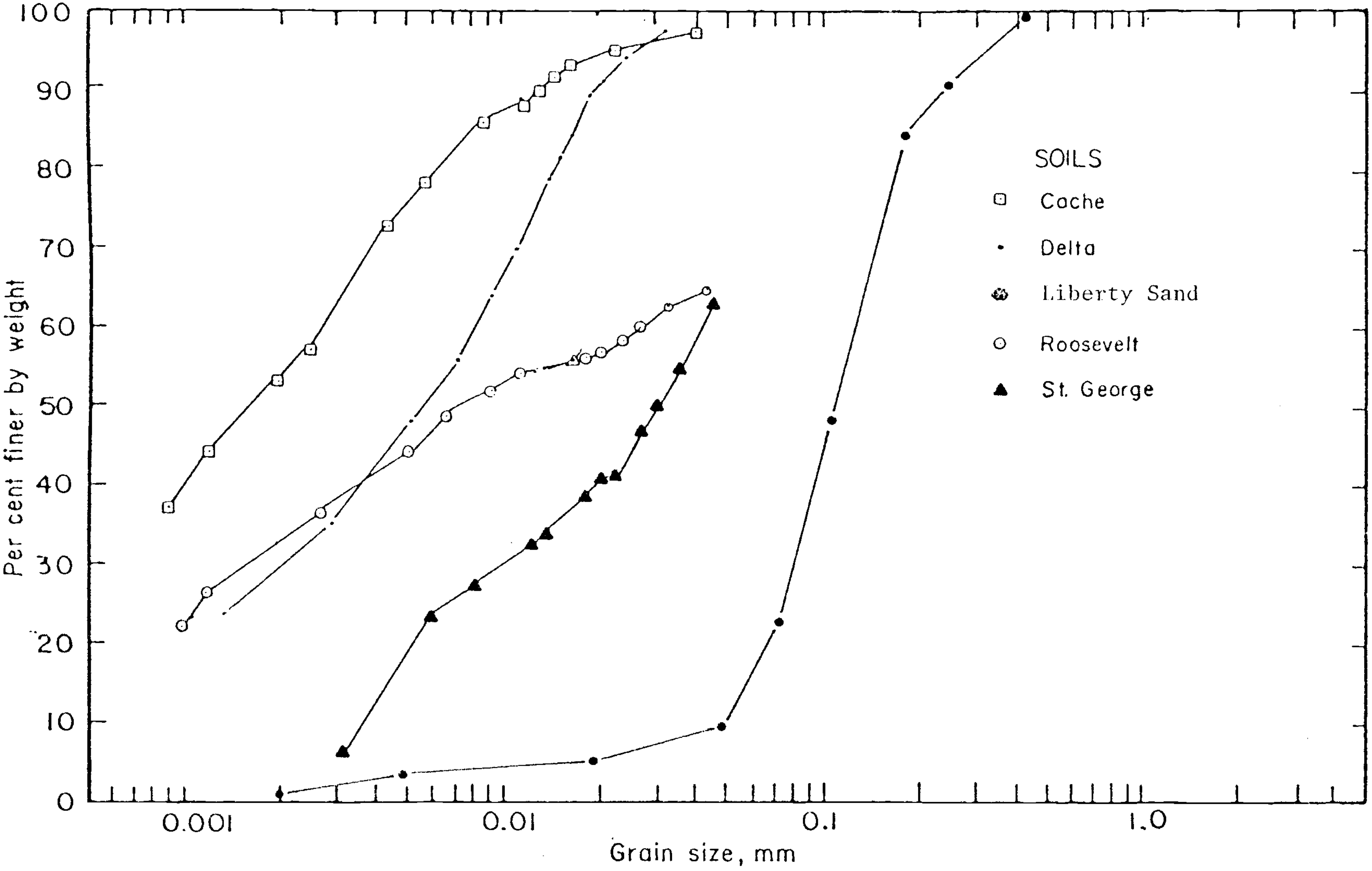

FIGURE 6. Utah State University Grain Size Distribution Curves [6,43].

each soil, while Table 2 identifies Atterberg limits for selected soils. An upward flow constant head permeameter (Figure 7) was used to evaluate: (1) the hydraulic gradient at which system failure occurred, (2) the plugging characteristics of the filter medium, and (3) soil bridging characteristics.

The hydraulic failure gradient of the system was determined by gradually increasing the flow rate until sample failure occurred. When the hydraulic failure gradient was exceeded, soil particles began migrating. This movement was accompanied by internal readjustment of soil particles and an associated reduced soil permeability and higher gradient at the same flow rate.

Table 2 identifies average hydraulic failure gradients ranging from 0.30 to 36 for the filter media and soils tested. One test was performed with soil, but no filter medium. A failure gradient of 0.75 was measured. For the same soil, with a fabric or screen, the failure gradient was approximately six. The importance of these results is that it was the soil that failed and not the filter fabric or screen. For the filter media tested, filter pore size appears to have virtually no effect on the hydraulic failure gradient. Coarse screens functioned as well as fabrics with small openings. In other words, after the minimum mechanical support has been provided for the soil by the fabric or screen, the mode of failure and the failure gradient are a function of the soil and not of the characteristics of the restraining material. Investigations did not identify the maximum pore size nor the minimum amount of load necessary to maintain this mechanical support.

TABLE 2. Soil Properties and Hydraulic Failure Gradients [6, 43].

Soil	D_{10} (mm)	D_{60} (mm)	C_u	C_z	PI	Hydraulic Failure Gradient Ref. 14	Hydraulic Failure Gradient Ref. 13
Cache	0.0002	0.0025	11.25	0.61	26	Over 36	50
Roosevelt	0.0004	0.0044	63.41	0.27	19	4.0	6.1
Delta	0.0005	0.007	15.47	0.92	16	3.5	3.5
St. George	0.0037	0.028	113.51	0.06	3	0.30	0.7
Liberty Sand	0.049	0.200	4.08	1.02	-	0.45	--

Notes:

All samples compacted under a pressure of 29.54 kN/m^2 with a No. 30 screen (opening size = 0.6 mm).

C_u = coefficient of uniformity = D_{60}/D_{10}

C_z = coefficient of curvature = $(D_{30})^2/(D_{60} \times D_{10})$

PI = plasticity index

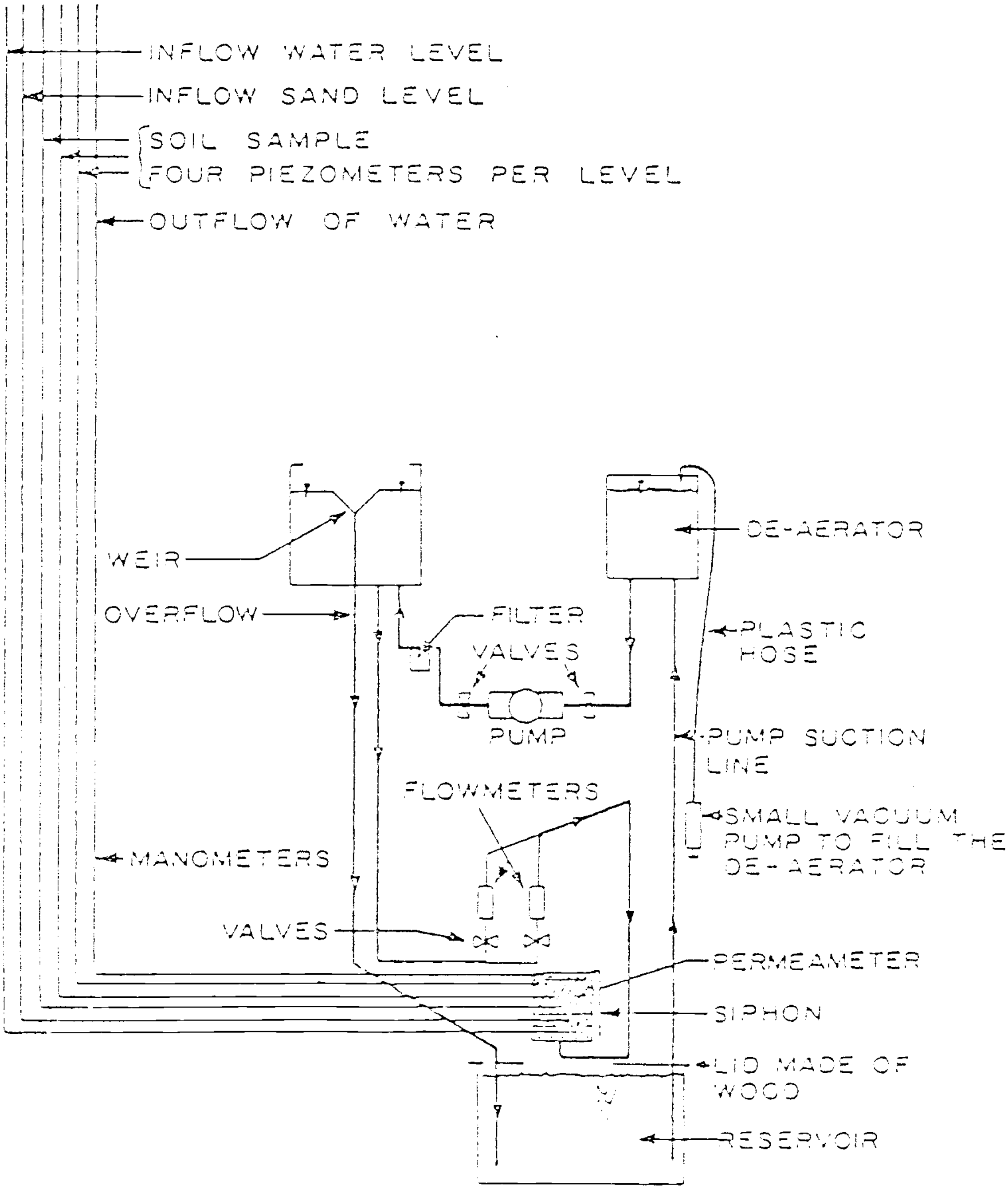

FIGURE 7. Utah State Upward Flow Permeameter [6, 43].

Similar conclusions can be drawn from tests conducted by Soil Testing Service, Inc. [3]). In this study, the effects of laminar vs turbulent flow conditions were investigated for two woven fabrics and three soil gradations. Turbulent flow was accomplished in the downward direction by increasing the hydraulic gradient to values beyond the Darcy flow regime. For the upward direction, a gradient greater than critical was applied through the soil that was unconfined at the filter outlet. In the downward direction (under turbulent conditions), soil particle migration was greater, but not excessively so. In upward flow (boiling occurring), soil loss of fine particles was excessive. Such a condition may be prevented by providing enough overburden to balance upward water forces such that silty and sandy soils are held in place. A conventional aggregate filter normally adds this weight. Similar results have been observed by other researchers [10, 31].

In the Utah State tests [6, 43], fabric plugging was observed after failure occurred. Plugging was observed by allowing the test to run for several hours after sample failure had occurred. The test was then concluded by reducing the flow to the original rate. The amount of plugging was expressed in terms of the difference in headloss at the beginning and end of each test. Observations indicated that the amount of plugging for a given soil and envelope material was dependent on the volume (flow rate times time) of soil reaching the fabric. In this case, it appears that the fabric is functioning as a true filter. That is, once the failure gradient has been exceeded, soil particles are essentially in suspension in the water. Therefore, the system can be expected to continue to plug and become less permeable. In these tests, plugging was not known to have occurred at gradients below failure.

Attempts have been made to identify soil properties that can be specified to select a fabric for a subdrainage installation. Batista [6] found that the hydraulic failure gradient correlated well with the plasticity index, as shown in Figure 8. Such a correlation is to be expected, since highly plastic soils (clays) will have strong interparticle attraction forces that will tend to minimize particle migration, as discussed earlier.

The above discussion of filtration theory has assumed intimate contact at the soil-fabric interface. It is apparent that neither piping nor plugging will occur if gradients remain below some failure point in this case. As mentioned earlier, intimate contact between the soil and fabric will not always be possible. Alternatively, if the hydraulic failure gradient is exceeded in the former case, the soil will become quick and intimate contact will no longer exist. In either event, soil particles will be suspended in water and the fabric will serve as a true filter. That is, the fabric will either become plugged and a soil cake will form, or piping will occur if the fabric pores are larger than the soil particles.

Filtering soil particles in suspension is analogous to cases of industrial and chemical filtration. Numerous studies have been conducted to evaluate the structure and performance of filter media [9, 11, 16, 18, 34, 42]. Grace [16] noted that when filtering suspensions that contain more than one percent by volume of solids, the pores block with a cake during the first few seconds or less and a continous cake

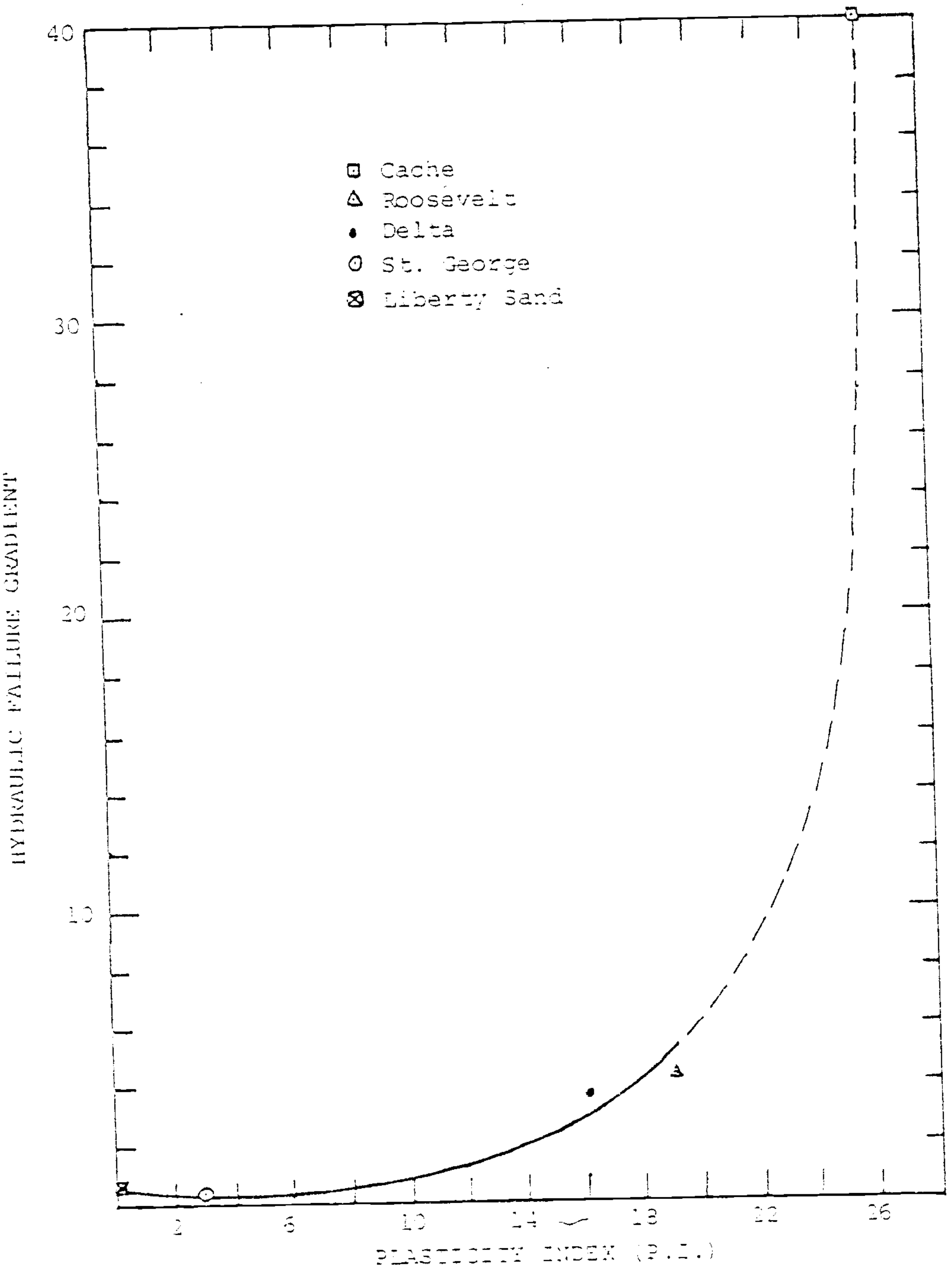

FIGURE 8. Relationship Between Plasticity and Hydraulic Failure Gradient [6].

covers the filter surface. This cake then serves as the active filter. Particle bridging across pores is expected to occur. Further, Hixon [18] suggests that the maximum pore over which bridging may occur may be expressed as:

$$d_p = 175\ \bar{d}^{\frac{1}{4}} \quad (2)$$

where: $\bar{d}$ = mean particle diameter, µm

d_p = pore size, µm.

Empirical relationships have been developed that relate pressure, filtrate volume, and time for hypothesized mechanisms of plugging. Although these mathematical expressions fit the experimental data for certain parts of the filtration cycle, there is no real evidence as to how pore blocking physically occurs. Tests used to filter 3 to 15 µ size particles suspended in 23 ppm by volume solution through woven fabrics indicated that only a microscopic cake had formed at interyarn pores and the yarn surface [16]. The significance of these results is that appreciable filtration is occurring through the yarn structure with cake formation mainly on the yarns.

Several relationships between permeability, pore size and porosity exist for granular soils [20, 37]. A common form of expression is:

$$k = A_1\ d^2 \quad (3)$$

where: k = coefficient of permeability

A_1 = constant, depending on geometric factors

d = some representative grain dimension.

Recently, Vaughan [41] was able to empirically develop a similar relationship between granular filter permeability and the size of the particle (δ) which will just pass the filter. By allowing clay particles suspended in water to pass through different granular filters, he found that:

$$k = 6.1 \times 10^{-6}\ \delta^{1.42} \tag{4}$$

where: k = coefficient of permeability of granular filters, m/s

δ = the largest particle that will pass, μm.

Vaughan [41] also reported that similar results were found by Lund [23] when using uniform base soils and filters of known permeability, and by Mantz [24] when using uniform quartz particles and both uniform and graded filters. Based on these results, it should be possible to develop a similar relationship, between fabric permeability and some soil particle size such that piping is minimized, of the form:

$$k = A_1\ \delta^{n_k} \tag{5}$$

where: n_k = a constant exponent.

Such an approach might eliminate the need for further measurements of fabric pore size.

Experience has shown that a conventional soil filter need only restrain the coarsest 15 percent of the soil. This has led to the relationship:

$$D_{15(filter)} \leq 5\ D_{85(soil)} \tag{6}$$

where: D_{15} = grain size for which 15 percent of the material is finer by weight

D_{85} = grain size for which 85 percent of the material is finer by weight.

To ensure free drainage, the filter must be much more pervious than the soil. This is accomplished when:

$$D_{15(filter)} \geq 5\ D_{15(soil)} \quad (7)$$

Numerous experimental studies have verified the above relationship [21, 36, 40].

In an attempt to relate fabrics to soil filters, the following relationship has been specified by several agencies [38]:

$$\frac{D_{85}}{\text{opening size of EOS (mm)}} \geq 1.0 \quad (8)$$

The EOS provides an indication of the maximum size opening of the fabric. It is determined by sieving (using successively coarser fractions) that size of uniform glass beads or sand grains of which five percent or less by weight passes through the fabric; the EOS is the "retained on" U.S. Standard Sieve number of this fraction [38]. Although several field installations built according to this specification have been successful, there is no physical reason as to why this requirement must be met, nor is there sufficient experimental evidence available to support or dispute its validity. Since the maximum size is determined by vibratory actions, it is not analogous to the steady movement created by groundwater flow. In addition, nonwoven fabrics with a wide range of pore sizes may be inaccurately represented by this one pore size. That is, the sieving action might identify one very large pore while some other size pore might better represent filtration behavior. Also, physical measurements might be hampered by electrostatic effects from glass beads coupled with bead entrapment in surface fibers. However, the EOS is probably a fairly good indication of pore size for a woven fabric with relatively uniform pores.

Permeability

In selecting a fabric for a subdrainage installation, both the fabric and soil permeability must be considered. Permeability is normally expressed in the form of Darcy's Law, assuming laminar flow. That is:

$$k = q/(i\ A) \tag{9}$$

where: k = coefficient of permeability

q = volume of flow per unit time

i = hydraulic gradient = $\Delta h/L$

where: Δh = head loss
L = thickness of fabric

A = cross sectional area.

In evaluating the effect of permeability on a subdrainage system, it will be necessary to identify the least permeable member, whether it is a plugged fabric or a soil cake.

Several studies have been conducted to evaluate the permeability of soil and fabric in direct contact when subjected to flow [8, 10, 25, 26, 31, 35]. Many of the studies reported a significant decrease in permeability with time. Four possible reasons might explain this behavior. First, air bubbles trapped in the pores commonly decreases permeability by reducing the pore volume available to flow. Second, if the particles are placed loose, rearrangement will occur under flow conditions, thereby reducing the pore volume, and as a result, the soil permeability. The third is the plugging of the fabric by soil particles. A fourth is the plugging of the fabric by the growth of organic matter. The first two and the fourth phenomena can develop in the soil irrespective of the presence of a fabric. The third possibility might occur if the hydraulic failure gradient is exceeded, thereby either clogging or binding the fabric.

Leatherwood and Peterson [21] have investigated the hydraulic head loss at the interface between uniform sands of different sizes by experiment. It was found that the hydraulic head loss at the interface is a function of the mean diameter of the smaller-sized material, the Reynolds number for flow through the smaller-sized material, and an empirical constant which appears to depend on the mean diameter and standard deviation of both materials. The relationship was expressed as:

$$h_L/D_s = C\ Re \qquad (10)$$

where: h_L = head loss at the interface

D_s = mean diameter of smaller sized material

C = empirical constant

Re = Reynolds number of the smaller sized material
$= v\, D_s/\nu_k$

where: v = flow velocity
ν_k = kinematic viscosity.

The one test involving a fairly well graded material yielded a relationship very close to the one above where D_s was represented by the mean particle size.

Perhaps the most amenable means of evaluating the permeability of a soil cake that might develop in a filtration situation is derived from the Kozeny-Carman relationship. Cake permeability (K_c) is expressed as:

$$K_c = \frac{\varepsilon^2}{K_k\, S_o^2\, (1 - \varepsilon)^2} \tag{11}$$

where: ε = porosity

S_o = specific surface
= particle surface area/particle volume

K_k = 2 to 5, depending on bed structure.

This relationship has been used in evaluating industrial filtration [7]. Inherent difficulties in this solution involve determination of the porosity and selection of an appropriate particle size from graded particles suspended in water. The ultimate effect on the overall soil-fabric system performance will also depend on the thickness of the cake that might develop.

In evaluating the ability of a fabric to transmit flow, either the coefficient of permeability or permittivity may be used. If permeability is specified, a thick fabric will be biased over a thin fabric [5]. That is, two fabrics of different thickness may pass equal quantities of water for the same conditions over a given amount of time, but have different values of permeability. Moreover, the effect of thickness on the overall soil-fabric system permeability may be insignificant since the fabric thickness is small relative to the soil thickness. As an example, consider flow across 10 cm (3.94 in) of soil, with a permeability of 10^{-3} cm/sec (2×10^{-3} ft/min), adjacent to a fabric. An equivalent soil-fabric coefficient of permeability (k_{eq}) can be expressed as:

$$k_{eq} = \frac{H_s + L}{H_s/k_s + L/h_f} \tag{12}$$

where: H_s = height of soil

L = thickness of fabric

k_s = coefficient of soil permeability

k_f = coefficient of fabric permeability.

For comparison, consider one fabric with a coefficient of permeability of 10^{-2} cm/sec (2×10^{-2} ft/min) and a thickness of 0.5 cm (0.2 in) and a second fabric with a coefficient of permeability of 10^{-1} cm/sec (2×10^{-1} ft/min) and a thickness of 0.3 cm (0.12 in). The corresponding equivalent coefficients of permeability would be 1.04×10^{-3} cm/sec (2.05×10^{-3} ft/min) and 1.03×10^{-3} cm/sec (2.03×10^{-3} ft/min), respectively. The effect of variations in thickness and k_f on k_{eq} indicate that a less permeable fabric might perform just as well as a more permeable fabric. Therefore, it appears that a technique should be adopted to measure the ability of a fabric to transmit flow that does not rely strictly on the coefficient of fabric permeability. Specification of permittivity is one method to consider. Permittivity is expressed as k_f/L, where L is the thickness of the fabric.

Although laminar flow is commonly assumed for flow through fabric, this may not always be the case. Turbulence may be identified when a linear relationship between velocity ($v = ki$) and hydraulic gradient no longer exists. The distinction between laminar and turbulent flow is illustrated in Figure 9. Darcy's Law may be modified as follows to account for turbulence [11, 30, 31]:

$$v^n = k\ i \tag{13}$$

where: k = coefficient of permeability

n = turbulence coefficient.

For laminar flow n has a value of one. Values of n greater than one are suggested by some degree of turbulent flow. Tests conducted at Delft Hydraulic Laboratories [31] involving upward flow through fabrics alone showed n to equal approximately 1.4. Further, permeability tests conducted on fabrics alone have shown turbulence to occur for conditions which might be experienced in practice. Others have found that the maximum gradient for laminar flow increased with increasing compression for needle punched fabrics [15].

Rollin [33] found that fabric permeability is related to the fiber density. Fabric permeability tests performed under a constant head of 35 cm (13.78 in) indicated that fabric permeability decreases with increasing fiber dentisy for thick nonwoven fabrics. A similar

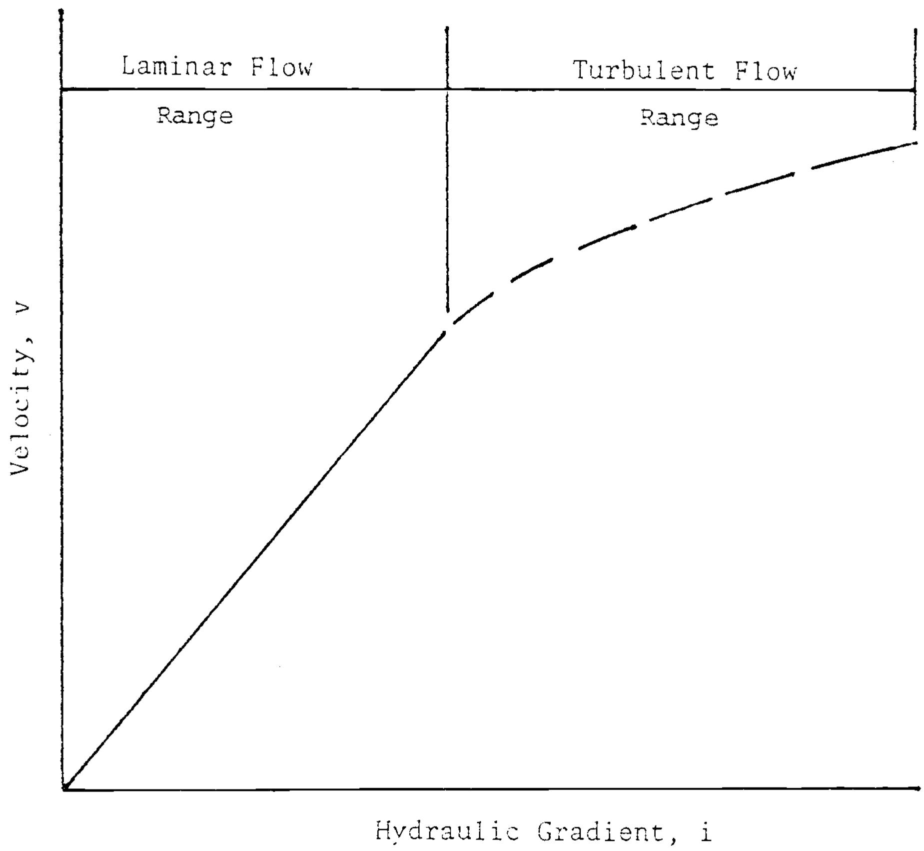

FIGURE 9. Laminar and Turbulent Flow

relationship for thin nonwoven or woven fabrics was not proposed but seems reasonable.

Summary and Evaluation

Two basic types of filtration have been identified: (1) where the soil is in direct contact with the fabric, and (2) where the fabric filters water containing suspended solids. Consideration of fabric types suggests that filtration behavior might be influenced by pore size, fiber diameter, and thickness. When intimate contact between the soil and fabric is maintained, a critical hydraulic failure gradient must not be exceeded. Maintenance of a gradient below this critical value will minimize particle migration or fabric plugging. Experimental evidence indicates that this hydraulic gradient is influenced by soil type and the mechanical support or overburden load on the filter. Fine sands and silts are the most failure-prone soils.

Gradients in excess of the failure value will require that the fabric function as a filter. In this case, or if dirty water is flowing, the fabric will either plug or particle migration will occur. Industrial and granular filtration studies have indicated that piping can be controlled by specification of the filter permeability, the maximum fabric pore size, and/or a particle size. Fabric specifications have related the EOS (an indication of the larger pore sizes) and the D_{85} size to minimize piping. However, it is questionable as to whether the critical gradient has been exceeded in installations built to this specification. Particle migration may occur at gradients beyond failure in installations built to this specification. A reduction in permeability attributed to fabric plugging and soil cake formation has been estimated from knowledge of particle size, the Reynolds number of the soil, and/or the porosity of the soil cake.

Much of the information presented thus far applies to industrial or granular filters. Industrial filtration generally occurs at greater pressure with relatively uniform particulate material in comparison to subdrainage filtration pressures and grain size distributions. Granular filters are normally much thicker than fabric filters. Based on these differences in filter thickness, pressures and filtrate characteristics, it appears that the following areas require further evaluation before fabric specifications can be defined.

(1) To minimize particle migration and fabric plugging, a means of predicting the critical hydraulic gradient from knowledge of grain sizes, fabric characteristics, and external loads requires further development.

(2) Constants involved in equations used to control piping in industrial and granular filtration through the specification of filter permeabilities, particle sizes and the EOS should be evaluated experimentally to determine their applicability to fabrics in subdrainage installations. These relationships include:

$$k = A_1 \delta^n , \qquad (5)$$

$$d_p = 175\, d^{-\frac{1}{4}} , \quad \text{and} \qquad (2)$$

$$\frac{D_{85}}{\text{opening size of EOS (mm)}} \geq 1.0 . \qquad (8)$$

(3) The influence of fabric permeability on subdrainage systems requires further definition.

(4) Methods to evaluate permeability reductions in terms of particle size, the Reynolds number of the soil, and/or the porosity of the soil cake due to fabric plugging or soil cake formation should be verified experimentally to determine their validity for fabrics in subdrainage installations.

Relationships to verify include:

$$k = \frac{\varepsilon^3}{K\,S_o^2\,(1 - \varepsilon)^2} \quad \text{and} \qquad (11)$$

$$h/D_s = c\ Re\ . \qquad (10)$$

Evaluation of these topics should indicate that fabric filter design requires the following information:

Fabric: Permeability and Pore Size

Soil: Grain Size

Flow Conditions: Hydraulic Gradient

External Conditions: Normal Stress on the Fabric

III. ANALYSIS

Prior to the development of test methods and subsequent design specifications, the mechanisms of filtration and the role of fabric permeability in subdrainage systems will be further analyzed. First, a method of predicting the critical hydraulic gradient will be proposed. Second, the influence of fabric permeability on trench drain performance will be evaluated with a hypothetical example.

Filtration Theory

For purposes of analysis, two types of filtration are considered. To review, these are:

(1) The soil is in direct contact with the fabric and clean water is flowing, and

(2) The fabric is filtering water containing suspended solids created either by exceeding the hydraulic failure gradient or by disturbances of soil fines during construction operations.

To evaluate the first type of filtration, recall the experimental studies conducted by Walker [43] and Batista [6]. It was found that, at increased gradients, small soil particles began to migrate. Further increases in the gradient caused either excessive particle migration or fabric plugging. Up to this failure gradient, it does not appear that fabric variations affect filtration performance. A better understanding of the arching phenomenon might simplify identification of the failure gradient for design purposes.

Figure 10 illustrates the steps involved in the development of an arch for upward flow in a cohesionless soil. The forces are identified as follows:

W_o - force on fiber from overburden

W'_s - effective weight of soil

F_s - seepage force at depth 7

As shown in Figure 10b, particle movement will occur first in Zone 1 when the seepage force (F_s) overcomes the effective weight of the soil (W'_s) and the soil becomes quick. This zone is not influenced by increased pressure due to the overburden. At this time, an arch will form by the remaining soil particles that are confined due to the overburden loads on the fibers. Further gradient increases will again cause particle movements as the seepage forces exceed the overburden forces (W_o) and the effective soil weight (W'_s). At this time, arches supported at the fibers may form or particle migration may occur. It is not clear whether failure is occurring at this time or if arches form after the soil becomes quick and continue to perform under increased gradients until a more severe failure occurs. It is anticipated that arch stability will depend on pore diameter and particle size. An equation relating the maximum pore diameterfor which arching will occur to a mean particle size (Equation 2) was given earlier as related to industrial filtration. Further investigation is needed to evaluate the stability of these arches in terms of pore size, particle size, and possible disturbance due to high gradients.

To evaluate the critical gradient where the soil becomes quick and begins to migrate from Zone 2, it is necessary to further define the

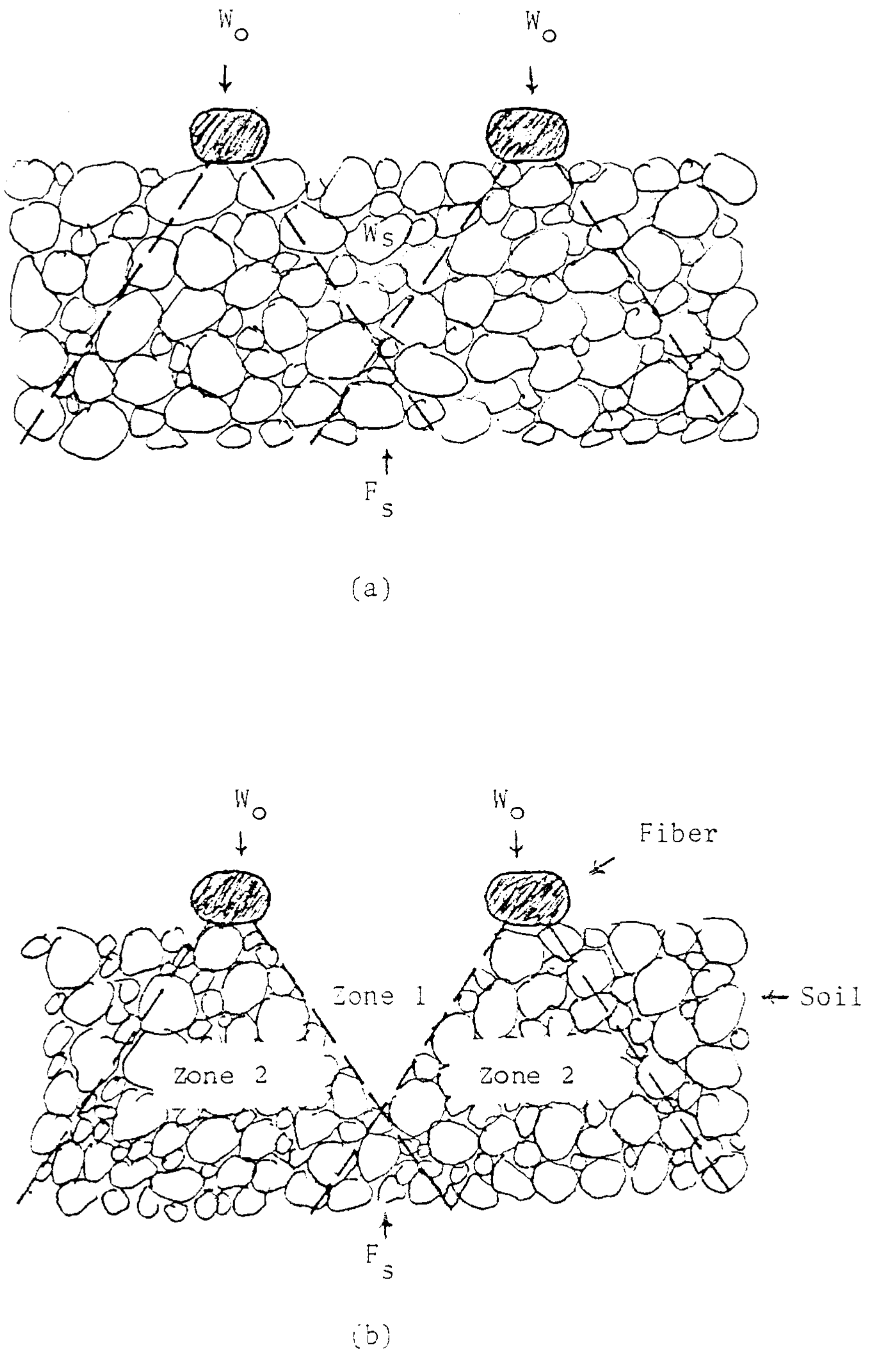

FIGURE 10. Upward Flow Filtration

forces involved. The overburden weight above the fabric will be assumed to be concentrated on the fibers. The pressure distribution beneath the fibers can be idealized, as shown by the dashed lines in Figure 10. By considering the fiber to be analogous to a ring-shaped footing, with an inner radius of r_i and an outer radius of r_o (i.e. r_i plus the fiber diameter), the stress distribution beneath the fabric pore center can be estimated using Boussinesq's method, as:

$$W_a = \int_{r_i}^{r_o} \frac{3\, q_o}{2\, \pi\, y^2} \frac{1}{\{1 + (r/y)^2\}^{5/2}}\, 2\, \pi\, r\, dr \qquad (14)$$

where: q_o = overburden pressure

y = depth below fiber level

W_a = pressure on soil from overburden above fabric at depth y.

Integrating:

$$W_a = q_o \left\{ \{1 + (r_i/y)^2\}^{-3/2} - \{1 + (r_o/y)^2\}^{-3/2} \right\} \qquad (15)$$

The overburden pressure (q_o) is calculated as:

$$q_o = (\gamma_a\, z\, A_T)/A_s \qquad (16)$$

where: γ_a = unit weight of overburden

z = depth of overburden

A_T = total fabric area

A_s = area of fabric fibers

This relationship may be further simplified by evaluating A_s in terms of the fabric porosity (n_p). That is:

$$A_s = (1 - n_p)\ A_T \tag{17}$$

Since:

$$n_p = 1 - \gamma/\gamma_f \tag{18}$$

where: γ = fabric unit weight

γ_f = unit weight of fabric solids.

then:

$$A_s = (\gamma/\gamma_f)\ A_T \tag{19}$$

Substituting Equation 19 into Equation 16:

$$q_o = \frac{\gamma_a\ z\ A_T}{(\gamma/\gamma_f)\ A_T} = \frac{\gamma_a\ z}{\gamma/\gamma_f} \tag{20}$$

This derivation of q_o has assumed that the overburden loads are concentrated on each fiber. This assumption is probably valid when the overburden material consists of grain sizes of the same order of magnitude as the fiber diameters and pores or if the fabric is rigid. However, if the overburden consists of much larger aggregate, there may be large fiber spans that are unsupported, as shown in Figure 11. The support from these fibers will depend upon the tension in the fabric that develops as the large aggregate deflect. Further analysis is required to better define this load distribution. However, as a first estimate, the present method of overburden evaluation is used to provide an approximation for critical hydraulic gradient predictions.

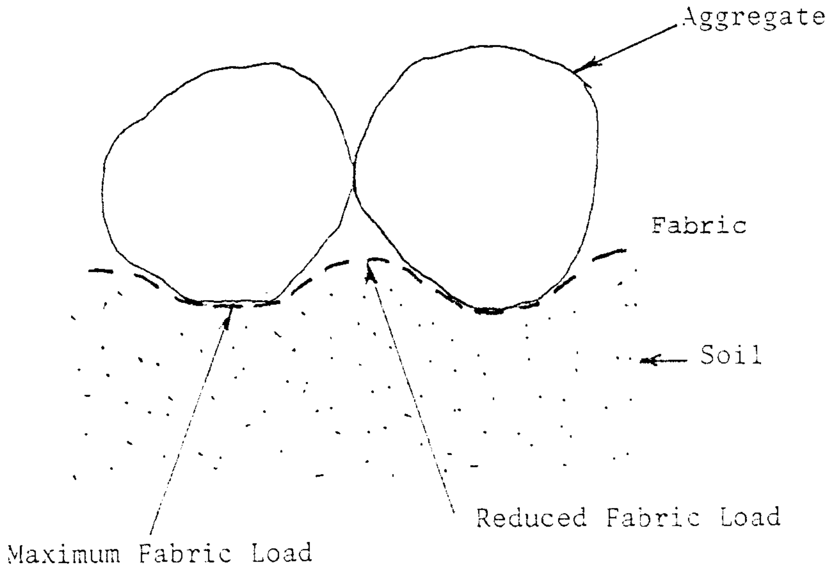

FIGURE 11. Importance of Aggregate Size on Fabric Loading

The seepage force (F_s) per unit area at the depth y can be evaluated as:

$$F_s = i \gamma_w y \tag{21}$$

where: i = hydraulic gradient

γ_w = unit weight of water.

The effective weight of soil per unit area at depth y may be evaluated as:

$$W'_s = y \gamma'_s \tag{22}$$

where: γ'_s = effective unit weight of soil.

As a conservative design measure, a subdrainage system might be designed to maintain the hydraulic gradient below the critical level. Theoretically, this could be accomplished by selecting a maximum gradient that yields a seepage force equal to the vertical downward force. That is:

$$F_s = W_a + W'_s \tag{23}$$

If a 2:1 slope (vertical:horizontal) for the overburden pressure distribution is assumed, then the deepest point in the "arch" will occur at $y = 2 r_i$. At this point, the gradient can be estimated as follows:

$$2i_c \gamma_w r_i = \gamma'_s 2r_i + \frac{\gamma_a z}{(\gamma/\gamma_f)} \left[0.716 - \{1 + (r_o/2r_i)^2\}^{-3/2} \right] \tag{24}$$

where: i_c = critical hydraulic gradient.

Solving for i_c:

$$i_c = \frac{\gamma_s'}{\gamma_w} + \frac{\gamma_a \, z}{(\gamma/\gamma_f) \; 2 \; \gamma_w \; r_i} \left\{ 0.716 - \; 1 + (r_o/2r_i)^2 \}^{-3/2} \right\} \qquad (25)$$

As previously mentioned, failure gradients greater than those calculated from Equation 25 might exist if a stable arch is able to develop. This critical gradient is only valid if the fabric pores are too large for arching to occur or if arches are unable to form after the soil becomes quick.

In the case of downward flow, the failure gradient will depend solely on the stability of the arches. Figure 12 illustrates the forces involved in downward flow. Some particle migration will occur prior to the formation of the arch.

The formation of this arch will, again, depend on the fabric pore size and the soil grain sizes. In addition, for this case, increases in the seepage pressure will result in an increase in the effective stress. Consequently, the shear strength would increase and may actually increase the stability of the arch. If this is the case, then the arch should never fail unless the seepage pressure is so large that it crushes the grains in the arch. Further investigation is required to investigate the stability of these arches.

Figure 13 illsutrates the forces involved in the event of horizontal flow. By considering the fabric to be analogous to a retaining wall, the horizontal forces are defined as:

W_p - passive force on fibers due to aggregate

E_o - at rest earth pressure

F_s - seepage force

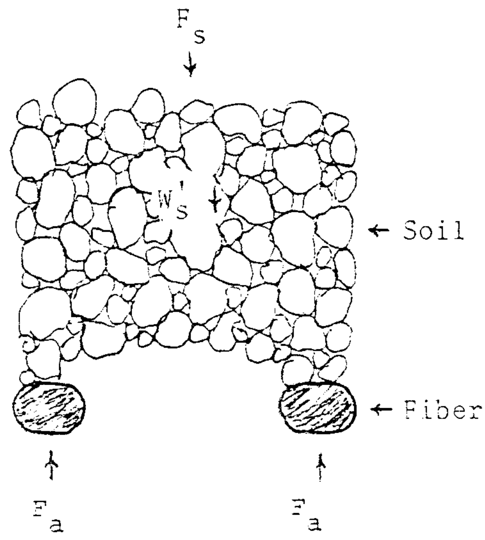

FIGURE 12. Downward Flow Filtration

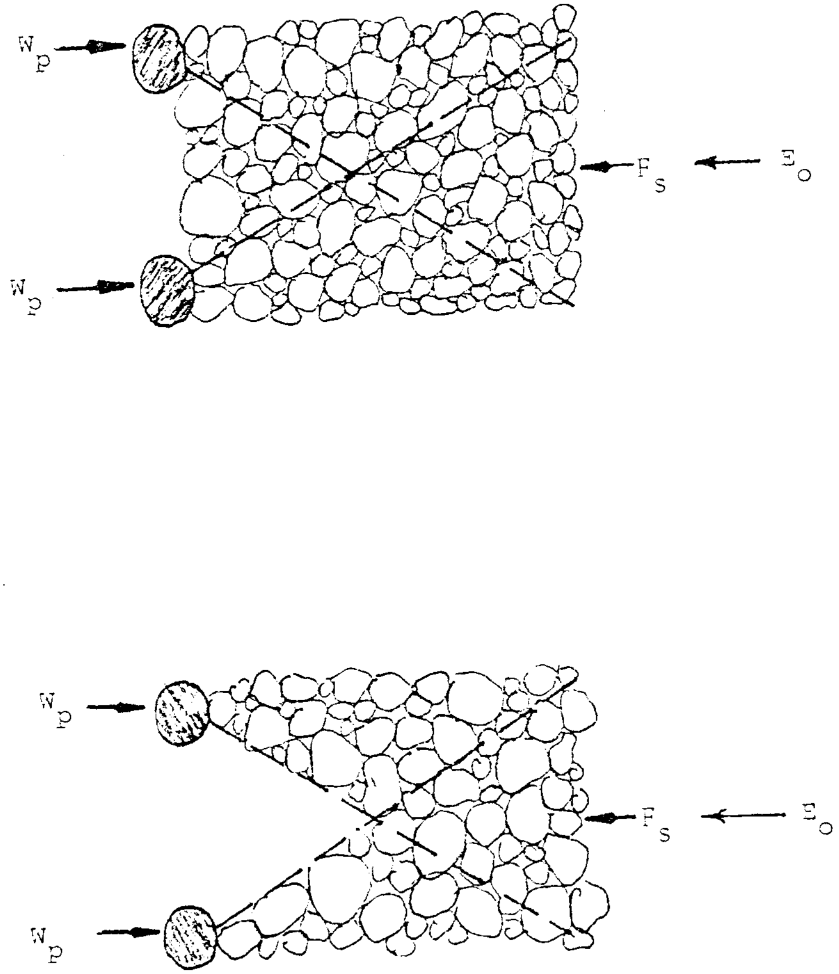

FIGURE 13. Horizontal Flow Filtration

In this case, a structural arch should form initially as unconfined soil particles leave the soil mass. As unconfined particles slough off, particles from above will move downward until they bear on other particles thereby forming an arch. As in the previous cases, the formation of this arch will probably depend upon the fabric pore size and the soil grain sizes. However, as with downward flow, gradient increases might serve to strengthen the arch unless grain crushing occurs. Experimental investigation is required to evaluate this hypothesized mechanism.

The above discussion has assumed intimate contact between the fabric and soil. If this cannot be guaranteed, then the fabric must be evaluated as a true filter. That is, either the fabric will plug or piping will occur. The formation of arches from suspended particles is uncertain at this time. Methods for evaluating this type of filtration were discussed in the Background Section.

Fabric Permeability

The role of fabric permeability in subdrainage performance has not been assessed. Fabric permeability may be expressed for one or both of the following reasons:

(1) To ensure that water can be removed without the buildup of excessive seepage forces and hydrostatic pressures, and

(2) To minimize particle migration.

Insufficient soil-fabric system permeability may result from either filter cake formation, fabric plugging, or insufficient initial permeability. Reductions due to the first two factors cannot be evaluated at this time without additional test data.

In the event that the hydraulic failure gradient is not exceeded and the water does not contain fines, the effect of fabric permeability on subdrain performance can be evaluated by considering the following example. Figure 14 identifies a trench drain with variables included in the analysis. These variables may be defined as follows:

x = distance from drain centerline to any point

x_f = distance from drain centerline to outer edge of fabric surface

x_d = distance from drain centerline to inner edge of fabric surface

h = height of seepage from drain base at distance x from drain centerline

h_f = height of seepage from drain base at distance x_f from drain centerline

h_d = height of seepage from drain base at distance x_d from drain centerline.

Flow across both soil and fabric is assumed to be laminar. In addition, the hydraulic gradient is assumed to be constant along a vertical section and equal to $\frac{dy}{dx}$ along the line of seepage. If a unit section of drain is considered, then

$$q = k \frac{dh}{dx} h \tag{26}$$

or:

$$q \; dx = kh \; dh \tag{27}$$

For any section, the height of seepage may be found by integrating between x_1 and x_2, h_1 and h_2. After integration and solving for h_2:

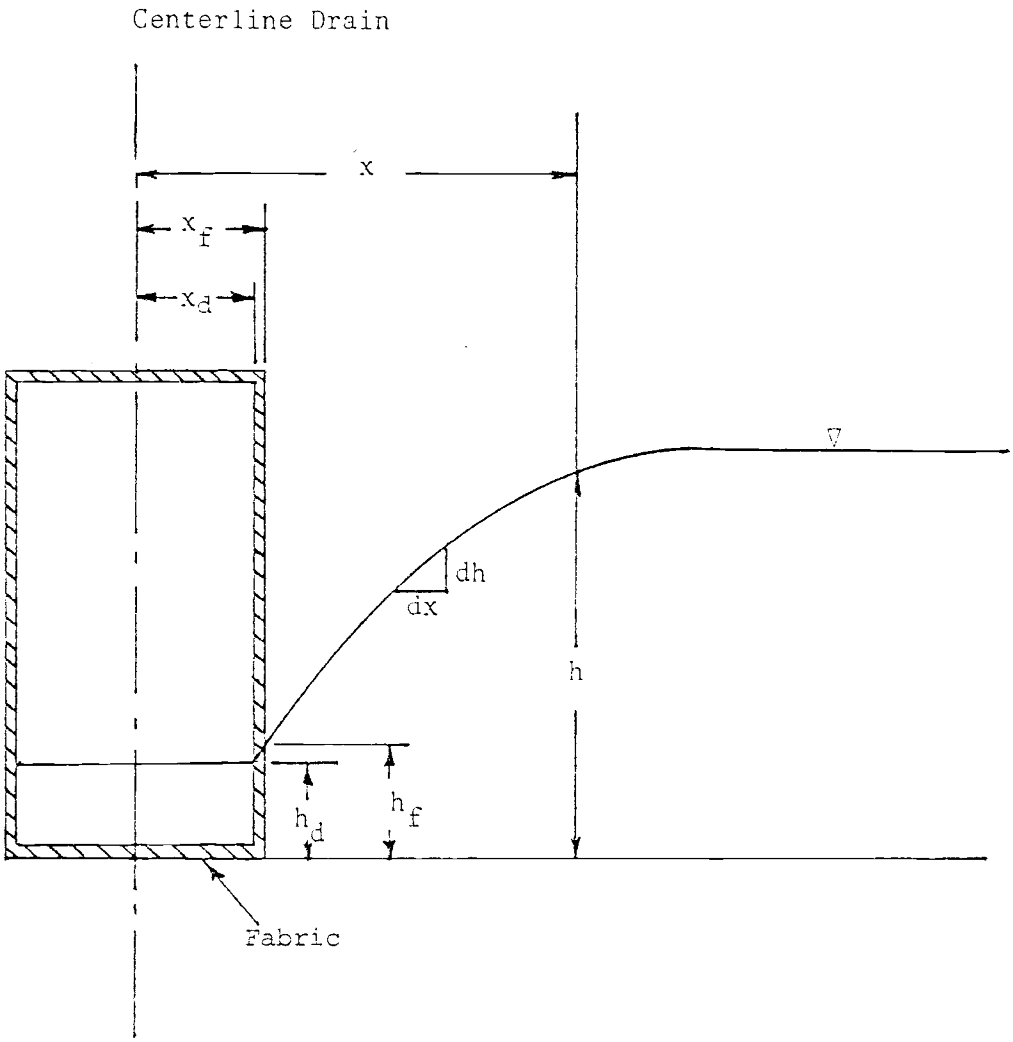

FIGURE 14. Trench Drain Variables

$$h_2 = \sqrt{\frac{2\ q\ (x_2 - x_1)}{k} + h_1^2} \qquad (28)$$

By evaluating this relationship between x_f and x_d the height of seepage at the outer fabric edge (h_f) is found to be:

$$h_f = \sqrt{\frac{2\ q\ (x_f - x_d)}{k_f} + h_d^2} \qquad (29)$$

Further evaluation between x_f and any point in the soil (x) reveals that:

$$h = \sqrt{\frac{2\ q\ (x - x_f)}{k_s} + h_f^2} \qquad (30)$$

As an example, consider the following:

q = .82 cm^3/sec (2.5 ft^3/day)

k_s = 10^{-3} cm/sec (2.83 ft/day)

h_2 = 65.58 cm (2.25 ft)

h_d = 9.14 cm (0.3 ft)

x_d = 18.29 cm (0.6 ft)

x_f = 18.36 cm (0.6025 ft)

For k_f values of 28.3, 2.83 and 0.283 ft/day, the entry point of water, h_f was 0.301, 0.307, and 0.366 ft, respectively. Figure 15 illustrates the effect of fabric permeability on the line of seepage in the soil, assuming a constant outflow. Note that the difference in h_f for $k_f = 0.1\ k_s$ and $k_f = k_s$ is almost ten times the difference between h_f

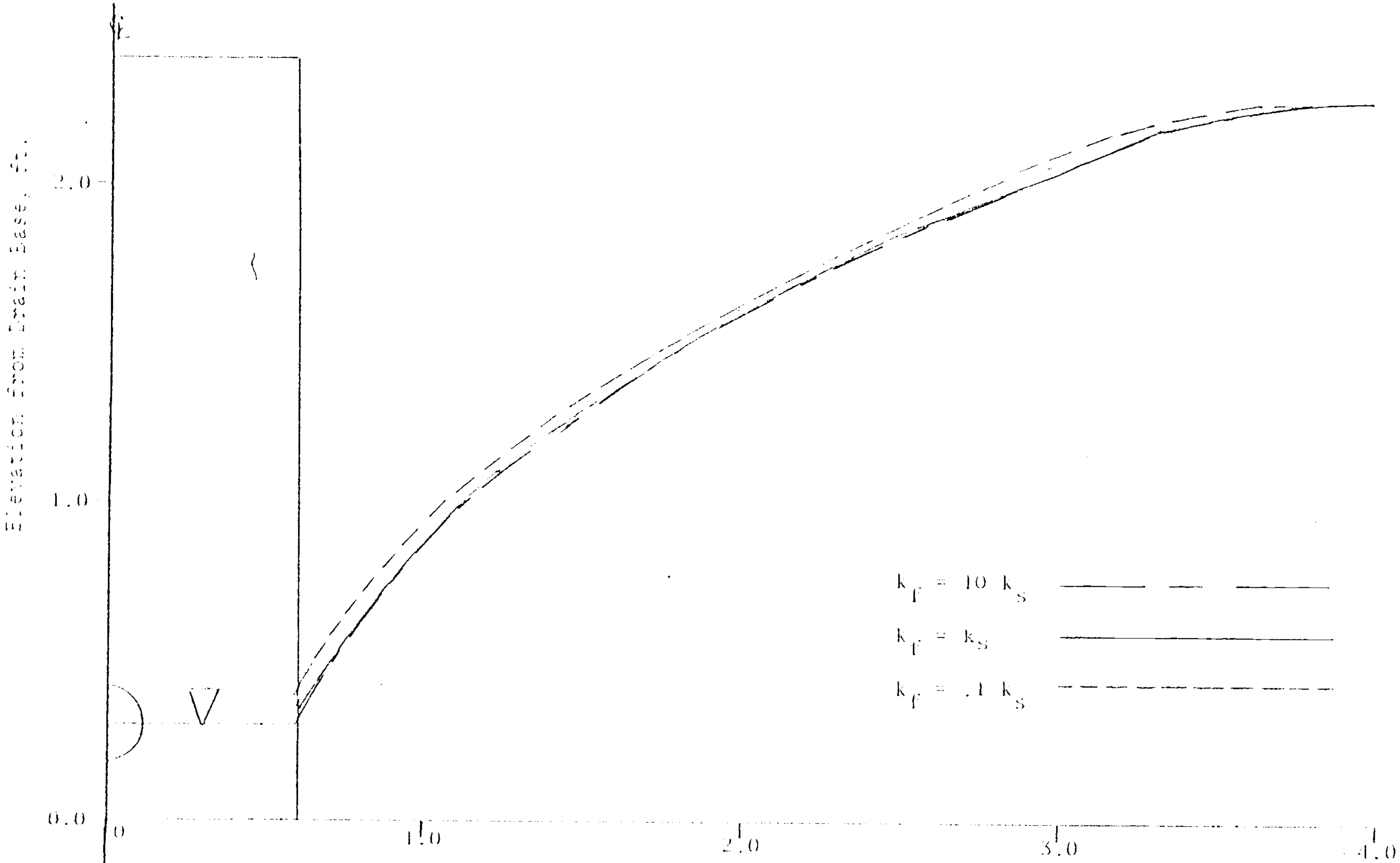

FIGURE 15. Effect of Fabric Permeability on the Line of Seepage

for $k_f = k_s$ and $k_f = 10\ k_s$. From this figure, it can be seen that the fabric permeability is not overly critical in terms of its effect on subdrain performance. For this example, it appears that for fabric permeabilities available on the market today (10^{-3} to 10^{-1} cm/sec (2.83 to 28.3 ft/day)), the fabric permeability does not affect the line of seepage significantly for a fixed flow ratio. Selection of the coefficient of fabric permeability should also be evaluated in terms of piping, as was discussed earlier. It should be emphasized that the above analysis does not include permeability reductions due to soil cakes or fabric plugging.

Summary

Analysis has shown that the critical hydraulic gradient is a function of the pore radius, the fiber diameter, the fabric weight, the unit weight of the soil, and the overburden pressure. The accuracy of this method of prediction should be evaluated experimentally.

The example used to illustrate the effect of fabric permeability on trench drain performance indicates that fabric permeability has a little influence on the line of seepage. Specification of a coefficient of fabric permeability must consider both the influence on hydrostatic pressures and seepage forces, and the influence on piping control.

IV. EXPERIMENTAL DESIGN

Experimental designs are proposed to further analyze the filtration mechanisms such that specifications can be developed to control particle migration, fabric plugging, and cake formation, and to predict the critical hydraulic failure gradient. Further, a method is developed to measure the fabric coefficient of permeability.

Filtration

Purpose and Scope

The filtration test series can be considered as having a two-fold purpose. First, in order to develop a means of estimating the hydraulic failure gradient for upward flow, tests should be run at overburden pressures typical of those that might be encountered in the field. The second purpose involves determining a relationship between filter fabric and soil characteristics, such that piping and/or plugging potential can be minimized. Flow conditions will be limited to upward and horizontal flow since they appear to present the most critical cases because of the uncertainty involved in the formation and stability of the arches.

Test Equipment

Both upward and horizontal flow tests should be performed under constant head conditions. Figures 16 and 17 illustrate schematic drawings for the upward and horizontal tests, respectively. Piezometers are installed on each side of the fabric (1 and 2), and at two locations

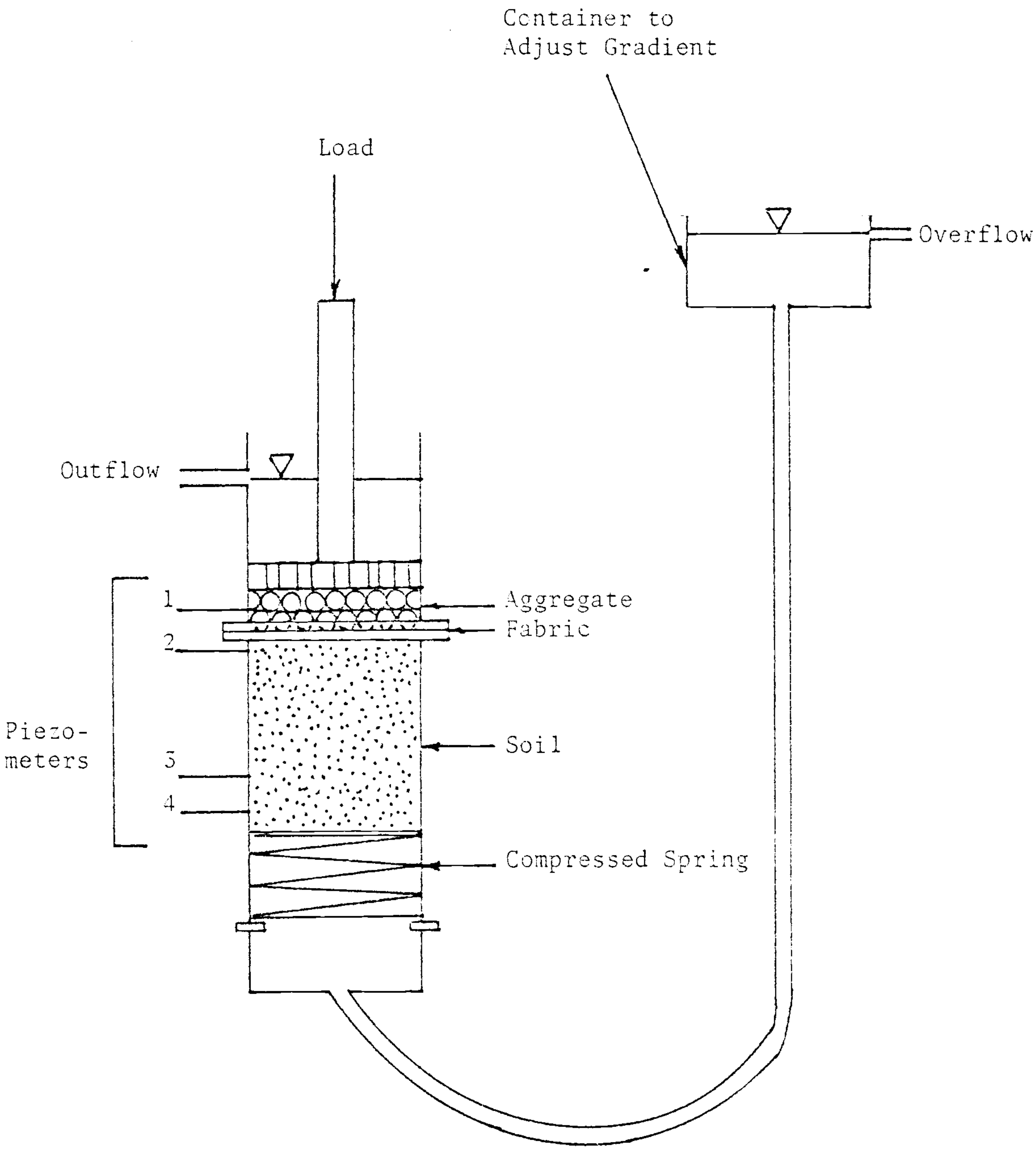

FIGURE 16. Upward Flow Schematic

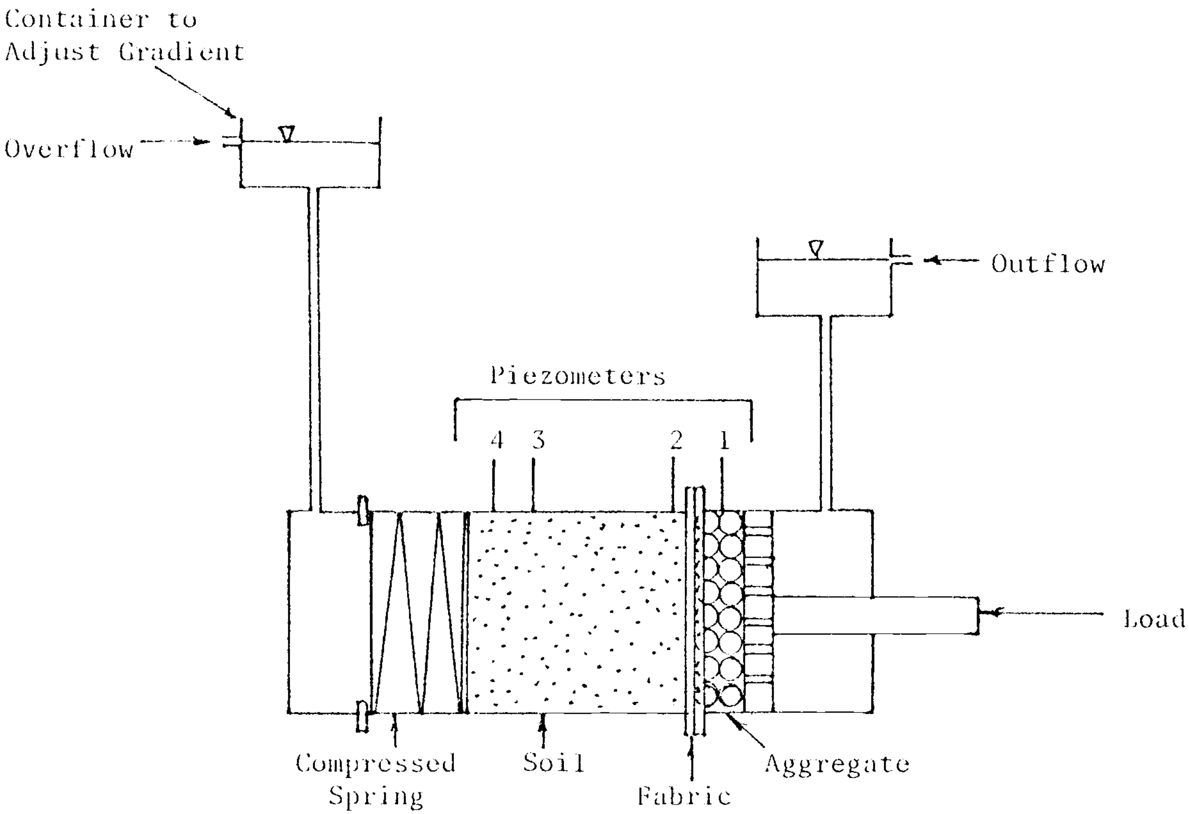

FIGURE 17. Horizontal Flow Schematic

several centimeters upstream in the soil (3 and 4). Head variance is accomplished by raising or lowering the attached container.

The soil and water should be deaired to eliminate reductions in permeability due to entrapped air. Distilled or filtered water should be used to eliminate fabric or soil plugging due to constituents in the water.

Test Procedure

Prior to soil placement, the soil should first be sterilized. This will ensure that any permeability reductions are not due to biological clogging that would occur regardless of the fabric's presence. The soil should be placed and compacted over a 170 g/cm^2 (350 psf) static load in 2.54 cm (1 in) lifts. This compaction process will simulate soil loading at a depth of about 91 cm (3 ft). Weight and volume measurements should be taken for density calculations.

To determine the hydraulic failure gradient, a given load is applied normal to the fabric surface. The head is then increased until failure occurs. Failure occurs as either piping or fabric plugging and/or cake formation. Piping will be visible as particles become visible in the water. Plugging or cake formation will be evident as the permeability between Piezometers 1 and 2 decreases relative to the permeability between Piezometers 3 and 4.

To evaluate piping or fabric plugging, tests will be performed at gradients beyond failure. Piped particles should be examined microscopically to determine what sizes migrate. Plugging must be examined by considering both soil and fabric permeability. By measuring the permeability of the virgin, as well as the plugged fabric and the permeability of the upstream soil at failure, an assessment of permeability reduction due to fabric or soil plugging can be made. Fabric permeability can be measured according to the falling test method, identified in the following section. To evaluate cake formation according to particle size, the material adjacent to the fabric should be microscopically examined to determine the size distribution.

To facilitate calculation of the coefficient of permeability, thickness measurements will be taken for each specimen. This procedure is identified in Appendix A. In addition, the EOS should be measured for possible correlation with a soil particle size to control piping. Table 3 summarizes information to be recorded during test performance for both failure gradient and piping-plugging tests.

Test Variables

To derive the maximum amount of information from a minimal amount of testing, the soils and fabrics listed in Table 4 were selected. The four fabrics and two screens were selected to cover a wide range of permeabilities and pore sizes and structures. The uniform soils were chosen to determine the effect of particle size variation without any influence from gradation. The gap graded soil was selected because it was thought that the fines might be more susceptible to movement, since velocities might be somewhat higher in the presence of the coarser material. The well graded materials were chosen so that a characteristic size might be identified for specification purposes in the event that the hydraulic failure gradient will be exceeded.

TABLE 3. Information to be Recorded for Filtration Tests

Soil	Soil Gradation Atterberg Limits Density
Fabric	EOS Thickness
Test Data	Piezometer Readings Total Head Loss Piped Particle Size Soil Cake Particle Size

TABLE 4. Soils and Fabrics to Test

Screens	No. 30 No. 60
Fabrics	Heat bonded nonwoven Needlepunched nonwoven Monofilament woven Slit-film woven
Soils or Glass Beads	(A) No. 30 - No. 40 (B) No. 60 - No. 70 (C) No. 100 - No. 120 (D) No. 230 - No. 270 (E) .01 - .005 mm 50% (A) + 50% (E) 25% (A) + 25% (C) + 25% (D) + 25% (E) 33% (C) + 33% (D) + 34% (E)

Load variations should be selected to simulate conditions likely to be encountered in the field. The following loads are recommended. Examples of where they might be encountered are also listed.

Load (psf)	Application
20	light cover for slope protection
120	load on blanket drain
300	load at base of average trench
1500	load at base of deep trench

An additional variable to be considered is the effect of time on piping, plugging, or soil cake formation. However, selection of test duration should be considered after initial test runs.

Analysis of Results

The hydraulic failure gradient as determined in the upward flow test can be compared to the value computed from Equation 25, as recited below:

$$i_c = \frac{\gamma_s'}{\gamma_w} + \frac{\gamma_a\, z}{(1 + \gamma/\gamma_f)\ 2\ \gamma_w\, r_i} \left\{ 0.716 - \{1 + (r_o/2r_i)^2\}^{-3/2} \right\} \qquad (25)$$

Comparison between these two values of failure gradient will confirm or refute the validity of the hypothesized mechanism of failure. A similar comparison can be made for the horizontal flow test.

Piped particle measurements will be applied in Equation 5, as recited below:

$$k = A_1\ \delta^{n_k} \qquad (5)$$

The value of k will be measured using the falling head test to be discussed later. By varying the fabric coefficient of permeability and the particle sizes, it is anticipated that values of A_1 and n_k can be determined such that particle migration can be evaluated for other combinations of fabric and soil. The value of A_1 may vary depending on fabric construction. Alternatively, a relationship between the D_{85} size of the soil and the EOS will be evaluated for woven materials.

Fabric plugging and cake formation will be quantified by two methods. However, prior to applying these two methods, it will first be necessary to determine if the reduction in permeability is due to the presence of the fabric, or if it would have occurred naturally in the soil as a result of increased gradients and the associated rearrangement of soil grains. The actual equivalent system coefficient of permeability can be calculated from the measured outflow (q) and the total head loss (Δh), as:

$$k_{eq} = \frac{q\ L_{sf}}{\Delta h\ A} \tag{31}$$

If permeability reduction is due to normal changes in soil structure, an unplugged equivalent permeability (k'_{eq}) can be calculated as:

$$k'_{eq} = \frac{L + H_{st}}{L/k_f + H_{st}/k_s} \tag{32}$$

where: H_{st} = total height of soil

k_f = coefficient of fabric permeability

k_s = permeability of soil between Piezometers 3 and 4
= $(Q\ L_{3-4})/\{A(h_4-h_3)\}$,

where: L_{3-4} = height of soil between Piezometers 3 and 4

h_4 = piezometer reading 4

h_3 = piezometer reading 3.

If $k'_{eq} = k_{eq}$, fabric plugging or cake formation due to the fabric has not occurred. That is, any reduction in permeability is due to normal changes in soil structure as a result of seepage forces.

In the event that permeability reductions are attributed to fabric-soil interactions, the plugged fabric permeability (k_{fp}), the soil cake permeability (k_c), and the extent of the soil cake (H_c) can be estimated. First, the plugged fabric is removed and the permeability is measured in the falling head test. Estimation of k_{fp} facilitates prediction of the head loss due to fabric plugging in the soil-fabric system. That is:

$$\Delta h_p = \frac{q\ L}{A\ k_{fp}} \tag{33}$$

where: Δh_p = head loss across plugged fabric, cm.

Since:

$$h_2 - h_1 = \Delta h_p + \Delta h_c \tag{34}$$

where: h_2 = piezometer reading 2

h_1 = piezometer reading 1

Δh_c = head loss across filter cake between Piezometer 2 and fabric.

the head loss across the soil cake can be estimated as:

$$\Delta h_c = h_2 - h_1 - \Delta h_p \tag{35}$$

The permeability of the soil cake (k_c) can then be calculated as:

$$k_c = \frac{q\ H_{c1}}{A\ \Delta\ h_c} = \frac{q\ H_{c1}}{A\ (h_2 - h_1 - \Delta\ h_p)} \tag{36}$$

where: H_{c1} = height of soil cake between fabric and Piezometer 2.

The extent of the filter cake can subsequently be estimated from:

$$k_{eq} = \frac{L + H_{c2} + H_s}{L/k_{fp} + H_{c2}/k_c + H_s/k_s} \tag{37}$$

and

$$H_{c2} + H_s = H_{st} \tag{38}$$

where: H_{c2} = total height of filter cake

H_{sa} = height of unaffected soil.

Substituting Equation 38 into Equation 37 and solving for H_{c2}:

$$H_{c2} = \frac{\{L + H_{st} - k_{eq}\ (H_{st}/k_s + L/k_{fp})\}\ \ k_c\ k_s}{k_{eq}\ (k_s - k_c)} \tag{39}$$

To quantify the filter cake permeability in terms of grain size and porosity, recall Equation 11:

$$K_c = \frac{\varepsilon^3}{K_k\ S_o^2\ (1 - \varepsilon)^2} \tag{11}$$

By measuring the filter cake particle sizes, S_o is obtained. Since k_c and S_o can be calculated, an estimate of the porosity can be found by solving for ε. If a limited range of porosities is found to exist, then a reasonable value of K_c could be estimated from Equation 11. This permeability can be converted to the soil cake coefficient of permeability as follows:

$$k_c = K_c \gamma_{20°C}/\mu_{20°C} \tag{40}$$

where: $\gamma_{20°C}$ = unit weight of water at 20°C (68°F)

$\mu_{20°C}$ = absolute viscosity of water at 20°C (68°F).

If the filter cake has a finite thickness regardless of soil thickness, then any decrease in permeability can be used to evaluate the overall performance of the subdrainage system.

In the event that a reduction in permeability is attributed to blinding at the soil-fabric interface, an approach such as Leatherwood and Peterson's [25] could be considered. That is:

$$\frac{h_L}{D_s} = C\ Re \tag{10}$$

The head loss (h_L) could be used to evaluate the plugged fabric permeability. Since the fabric coefficient of permeability is related to piping potential, then it may also be related to the particle size that just blinds the fabric surface. However, it should be noted that blinding will be difficult to identify, since particles may become dislodged as the fabric is removed from the soil.

Either method of evaluating reductions in permeability requires knowledge of a soil grain size. It is anticipated that just as particle migration is related to the fabric permeability, so the soil cake grain size will have some relationship to the fabric permeability.

Use of Results

The proposed filtration test plan is designed with the intent of providing information for the development of specifications. More specifically, verification of the equation for the critical hydraulic gradient will enable the designer to select a fabric in terms of the maximum pore size, the soil unit weight, and the overburden load, provided intimate soil-fabric contact is assumed. Selection of a fabric with Equation 25 will assure minimal particle migration and fabric plugging.

If particles are suspended in water, then particle migration and/or fabric plugging must be controlled. If it is determined that fabric plugging and/or cake formation occur to only a limited extent and the effect is not detrimental to the overall subdrain performance, then the allowable reduction in permeability can be used to estimate the soil cake particle size (Equations 10 and 11). This value can then be used to select the fabric coefficient of permeability.

If it is found that the reduction in permeability due to plugging or soil cake formation is excessive or continues to worsen with time, then plugging or soil cake formation must be controlled by allowing piping to occur. This can be accomplished through the specification of fabric permeability, according to Equation 6. In both cases, a representative grain size must first be identified.

Permeability

Permeability tests were performed such that a reliable means of measuring the water transmissibility of a fabric could be developed.

Air permeability was determined for comparison to falling head test results. Twenty-two fabric types were tested.

Air permeability tests were performed in accordance with ASTM D-737 [36]. All fabrics were tested with a pressure drop of 1.27 cm (0.5 in) of water across the fabric. The flow rate was recorded in cfm/ft^2 after measuring the pressure of the outflow in inches of water. For each fabric, a minimum of seven samples was tested.

A falling head test was used to measure the ability of the fabric to transmit water flow. The test apparatus consisted of a 5.08 cm (2 in) diameter cylinder with a 2.54 cm (1 in) opening at the flanges, as shown in Figure 18. The fabric was clamped between the flanges with six bolts. After sealing all openings, a vacuum of 64 cm (25 in) of mercury was applied to the permeameter. This step was to ensure that air did not remain entrapped within the fabric. The permeameter was filled with deaired, distilled water from the bottom with the vacuum applied. After recording the temperature, the time was recorded for the water level to fall from 30 cm to 10 cm (11.8 to 3.9 in) above the fabric. For each fabric, seven samples were tested. The number of timings for each sample was determined after performing seven runs on the first sample. Using a Student's t distribution, the number of runs with one sample required to yield a timing within five percent of the true mean with a 95 percent probability is [32]:

$$n_t = 0.154\ \nu^2 \tag{41}$$

where: n_t = number of timings required

ν = coefficient of variation, percent.

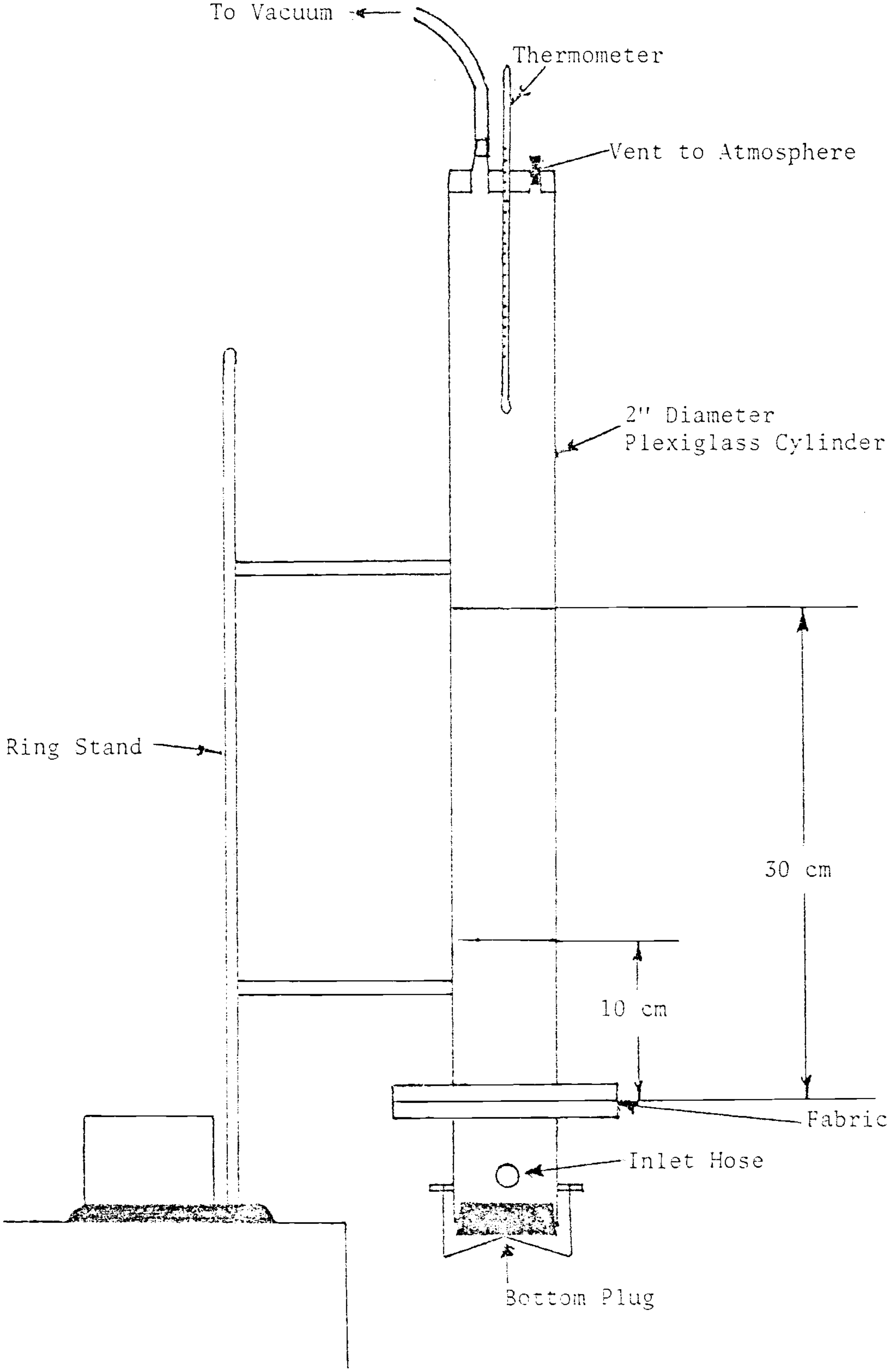

FIGURE 18. Schematic of Falling Head Test Apparatus

A more detailed test procedure can be found in Appendix A.

Thickness was measured according to the procedure described in ASTM D-1777 [1] except that a 125 g load was applied over a 25 cm^2 foot that rested on the fabric. These values were selected such that a nominal pressure could be applied over a fairly large area to minimize fabric compression and allow for fabric irregularities.

Table 5 identifies fabric types tested. Identified are nominal weights, fiber content, and manufacturing process. These fabrics were selected to represent a range of types and weights available on the market today.

Permeability was calculated as:

$$K = \frac{\mu L}{q A \Delta P} \tag{42}$$

where: K = permeability

μ = absolute viscosity of air at 21.1°C (70°F)

L = fabric thickness

ΔP = pressure drop across fabric

A = cross sectional area

q = discharge per unit time.

To convert to water permeability:

$$k_a = \frac{\gamma_{20°C}}{\mu_{20°C}} K \tag{43}$$

where: k_a = coefficient of fabric permeability computed from air permeability results

TABLE 5. Fabrics Tested for Permeability

Identification Number	Fiber Polymer(s)	Construction	Nominal Weight gm/m2 (oz/yd2)
NONWOVEN			
NW-1 (3)	Polyester	Resin bonded Staple filaments	80 (3.5)
NW-2 (4)	Polypropylene and Polyamide	Heat bonded continuous filaments	95 (4)
NW-3 (4)	Polypropylene	Heat bonded continuous filaments	95 (4)
NW-4 (8)	Polyester	Needlepunched continuous filaments	190 (8)
NW-5 (17)	Polypropylene	Needlepunched continuous filaments	400 (17)
WOVEN			
W-1 (4)	Polypropylene	Woven slit film	95 (4)
W-2 (7)	Polypropylene	Woven multifilament	170 (7)
W-3 (8)	Polyamide	Woven multifilament	190 (8)
COMBINATION			
C-1 (4)	Polypropylene	Woven slit film with needlepunched nap	95 (4)

To minimize biassing a thick fabric over a thin fabric based on permeability, the permittivity is expressed as:

$$k_{ap} = k_a/L \tag{44}$$

where: k_{ap} = permittivity determined from air permeability.

The number of fabric samples required to yield a mean value of q within five percent of the true mean with a 95 percent probability was calculated assuming a Student's t distribution, as given in Equation 45. Values were also calculated for probabilities of 90 and 80 percent, as given below.

Probability	Number of Samples Required	
95	$0.154\ \nu^2$	(41)
90	$0.108\ \nu^2$	(45)
80	$0.066\ \nu^2$	(46)

The fabric coefficient of permeability was calculated from falling head data, and was expressed in the following form:

$$k_f = \frac{a\ L}{A\ t}\left(\ln \frac{h_1}{h_2}\right)\frac{\mu_T}{\mu_{20}} \tag{47}$$

where: k_f = coefficient of fabric permeability

a = area of cylinder

A = area of fabric specimen

t = time for water level to fall from h_i to h_f

h_i = height of water at beginning of test

h_f = height of water at end of test

μ_T = absolute viscosity of water at test temperature

μ_{20} = absolute viscosity of water at 20°C

L = fabric thickness

Permittivity was subsequently calculated as:

$$k_p = k_f/L$$

where: k_p = permittivity determined from falling head test results.

For each fabric, the number of samples required to obtain a mean value of the fabric coefficient of permeability within five percent of the true mean at a probability level of 95, 90, and 80 percent was calculated using Equations 41, 45, and 46 respectively.

V. RESULTS

Test results are presented for air and water permeability tests only. Table 6 gives results from air permeability tests performed. Table 7 identifies falling head test results. Statistical results for both methods, including maximums, minimums, means, standard deviations and the number of samples required to achieve a given accuracy can be found in Appendix C. Thickness data are also summarized in Appendix C. Sample calculations of test results are presented in Appendix B.

Generally, nonwoven fabrics were characterized by larger coefficients of permeability than the woven fabrics. Coefficients of permeability from falling head tests (k_f) ranged from 1.6 x 10^{-3} cm/sec to 3.78 x 10^{-1} cm/sec (3.1 x 10^{-3} to 0.74 ft/min). Permittivity values ranged from 0.03 to 1.44. The importance of specifying permittivity is best supported by considering two fabrics of different permeabilities. As an example, fabric NW-4 (8) (k_f = 3.38 x 10^{-1} cm/sec) is about four and one half times as permeable as NW-2 (4) (k_f = 0.73 x 10^{-1} cm/sec), but both have the capacity to pass nearly the same quantity of water per unit time with permittivities of 1.15 sec^{-1} and 1.07 sec^{-1}, respectively.

The coefficients of fabric permeability calculated from air permeability test data (k_a) tended to be about twice the values of the coefficient of fabric permeability (k_f) computed from water permeability test data. Figure 19 illustrates the relationship between permittivities ($k_f/\bar{L}$) determined from the falling head and the air permeability tests.

TABLE 6. Air Permeability Test Results.

Fabric Number	Flow Rate $ft^3/min/ft^2$	Coefficient of Permeability, k_a cm/sec x 10^2	Permittivity, k_a/L 1/sec x 10
NONWOVEN			
NW-1 (3)	357.4	22.1	25.9
NW-2 (4)	300.5	15.8	21.8
NW-3 (4)	79.0	2.18	5.73
NW-4 (8)	295.7	64.3	21.5
NW-5 (17)	175.8	65.5	12.8
WOVEN			
W-1 (4)	7.2	0.29	0.52
W-2 (7)	142.8	4.18	10.4
W-3 (8)	9.6	0.34	0.69
COMBINATION			
C-1 (4)	27.1	1.90	1.97

Note: 1 $cm^3/sec/cm^2$ = 1.969 $ft^3/min/ft^2$

1 cm/sec = 0.0328 ft/sec

TABLE 7. Falling Head Test Results

Fabric Number	Coefficient of Permeability, k_f cm/sec x 10^2	Permittivity, k_f/L 1/sec x 10
NONWOVEN		
NW-1 (3)	12.3	14.4
NW-2 (4)	7.8	10.7
NW-3 (4)	1.28	3.36
NW-4 (8)	33.8	11.5
NW-5 (17)	37.8	7.39
WOVEN		
W-1 (4)	0.20	0.36
W-2 (7)	1.79	4.47
W-3 (8)	0.16	0.33
COMBINATION		
C-1 (4)	1.07	1.11

Note: 1 $cm^3/sec/cm^2 = 1.969\ ft^3/min/ft^2$

1 cm/sec = 0.0328 ft/sec

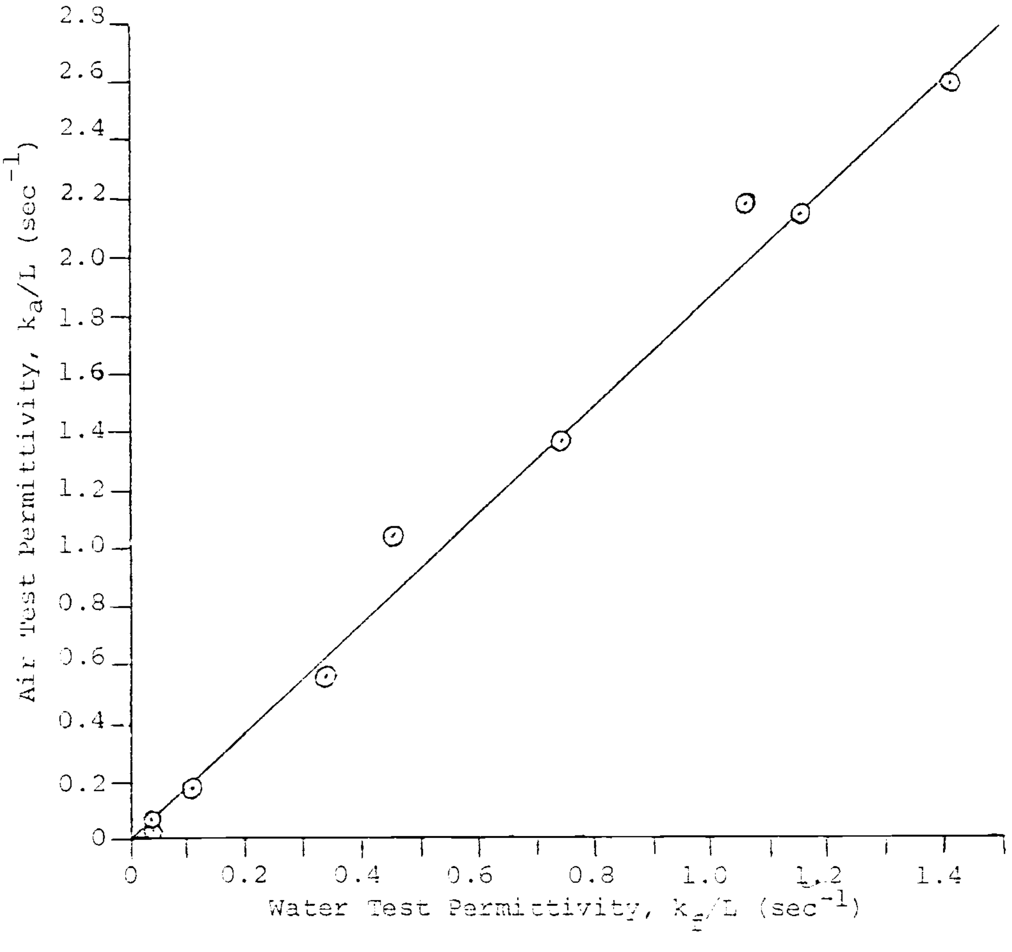

FIGURE 19. Relationship Between Air-Test Permittivity and Water-Test Permittivity

The effect of thickness on the fabric coefficient of permeability is illustrated in Figure 20. These data were obtained from tests run with from one to five layers of fabric. As the number of fabric layers increased, the coefficient of fabric permeability increased and then became constant at about twice the value of one layer.

Table 8 compares the variations in the air flow rate that might occur as a result of different methods of sample selection. Note that large differences in air flow rates existed between lots. Only small differences in air flow rates existed for samples taken from the same lot but selected by different methods. As indicated by Table 9, operator variance for the falling head test is not likely to significantly affect calculated values of the coefficient of fabric permeability (k_f). Calculated values of k_f varied by no more than seven percent.

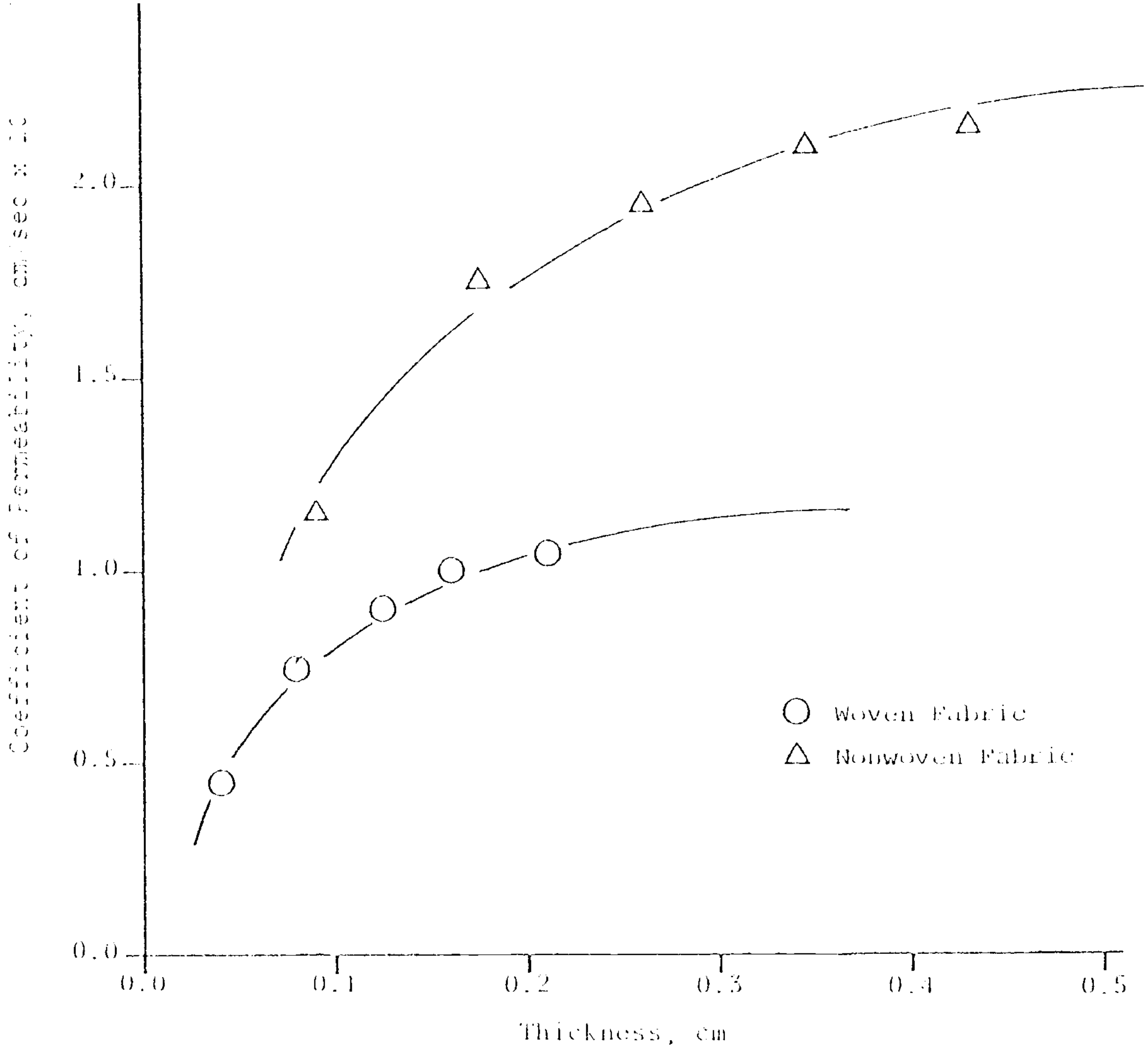

FIGURE 20. Relationship Between Fabric Thickness and the Coefficient of Permeability

TABLE 8. Effect of Sample Selection on Air Permeability Results

Fabric Samples		Mean Flow Rate $ft^3/ft^2 \cdot min$	Standard Deviation	Coefficient of Variation, %	Number of Samples Tested
NW-4 (4)	A	458.3	49.80	10.87	7
	B	425.6	43.32	10.18	7
	C	319.7	12.03	3.76	5
W-2 (7)	A	146.2	18.5	12.7	7
	B	147.4	15.68	10.64	7
	C	109.4	34.77	31.78	5
NW-3 (6)	A	23.3	1.85	7.92	7
	B	20.6	3.00	14.57	7
	C	27.5	4.47	16.30	5

Note: A and B were taken from the same lot. The A samples were cut from one small area. The B samples were randomly selected from a large area. The C samples originated from a different fabric lot.

TABLE 9. Effect of Operator Variance on Falling Head Test Results on One Fabric Specimen.

Operator	A	B	C
Mean (viscosity/time)	0.2994	0.3001	0.3180
Standard Deviation	0.0087	0.0143	0.0077
Coefficient of Variation	2.91	4.77	2.42
Number of Timings	7	7	7
Calculated Permeability, k_f (cm/sec)	0.113	0.114	0.120

VI. DISCUSSION

The fabric coefficient of permeability is specified for one or both of two reasons: (1) to prevent the buildup of seepage forces, and (2) to control particle migration and fabric plugging. While the required fabric coefficient of permeability for a given soil cannot be specified at this time prior to completion of the proposed filtration test plan, discussion will focus on the development of a suitable test for its measurement for later use. Sample variability, lot variability, the influence of the number of fabric layers, operator variability, problems encountered during test development, falling head test design features, and ease of test performance will be considered.

The falling head test equipment was dimensioned with a 5.08 cm (2 in) diameter standpipe and a 2.54 (1 in) diameter fabric opening for two reasons. First, to enable fabric deairing to be accomplished in a minimal amount of time and to minimize the amount of deaired water required, a relatively small volume was required. The second criterion for dimensioning was to ensure that a reasonable amount of time would elapse as the water fell between two points for all types of fabric tested. The time had to be long enough so that a reading could be taken with reasonable accuracy not overly influenced by human reactions. In addition, large times were undesirable, since this would reduce test efficiency. The problems of deairing and time measurement could be solved by a number of modifications. First, a larger diameter standpipe would increase the time. However, this would increase the required amount of deaired water. Second, for a smaller diameter standpipe, a larger head drop could be specified. Although this could increase times without undue increases in water requirements, a physical restraint would be imposed to record short times at points widely spaced. The third, and selected, alternative was to choose a standpipe diameter with a smaller fabric opening. This scheme effectively increases test times without an increase in deaired water requirements. With a head drop between 30 and 10 cm (11.81 and 3.94 in) and a 5.08 cm (2 in) diameter standpipe accompanied by a 2.54 cm (1 in) diameter fabric opening, an acceptable range of times was found between 1.5 and 50 seconds. Another modification that would enable very short times to be recorded with no human error would be the installation of an electronic timer connected at the top and bottom water levels. This approach to time measurement appears to be the most feasible. However, time did not permit development of this technique for this study.

To eliminate the effect of any back pressures developed beneath the fabric during test performance, a quick opening system at the base was necessary. The rubber stopper scheme effectively fulfilled this need. In addition, a further guarantee that any back pressures would be relieved could be accomplished by initially filling the permeameter above the top test line. By filling the permeameter 10 cm (3.94 in) above the top line, free flow during test performance was guaranteed. This step also ensured adequate time to accurately begin recording the time at the top line.

The decision to use deaired water was made to eliminate variations in test results due to varying quantities of entrapped air within the fabric and water. In addition, this action eliminated any need for prewetting the samples. Prewetting is commonly applied to ensure saturated samples. However, for some samples, a fiber coating makes this process difficult. For samples of this type, the deairing process eliminated increases in the fabric coefficient of permeability as more tests were run and the sample became more fully saturated. Therefore, the use of deaired water and fabric should be adopted to eliminate the problems of prewetting necessary to remove air and to ensure consistent test results.

Water temperature variations are known to have a significant effect on the coefficient of permeability. As the temperature increases, the viscosity of the water decreases, resulting in an apparent increase in the coefficient of permeability. To standardize all results at one temperature, the coefficient of permeability is corrected for viscosity by multiplying k_f at test temperature by the ratio of the viscosity at the test temperature to the viscosity at the standard temperature. The standard temperature was chosen as 20°C (68°F).

Water permeability tests should be performed with distilled or filtered tap water. During the early stages of testing, it was noticed that the fabric became discolored with successive test runs. Tap water impurities would serve to plug the fabric with time, resulting in a lower coefficient of fabric permeability. This effect should be eliminated by using distilled or filtered tap water.

Table 3 identifies the effect of sample selection on air permeability test results. For two of the three fabric types, the coefficient of variation was essentially independent of where samples were cut, provided that they were taken from the same lot. However, for the other fabric, the coefficient of variation was much greater when samples were selected randomly over a large area, rather than when taken from one localized area. This finding indicates that since fabric variability is high over a large area, samples should be cut over a large area to obtain a representative value of permeability.

The variation in air permeability results between different lots of fabric is also exemplified in Table 8. In all cases, there is a 30 to 45 percent variation in the mean flow rate between lots. In addition; for two cases the higher flow rates corresponded to fabrics with greater thicknesses. This combination of high flow rates and greater thicknesses results in even greater variability between coefficients of permeability. For example, the coefficient of permeability varied by almost a factor of three between lots for NW-4 (4). Therefore, it cannot be assumed that the mean permeability will be constant for all fabric lots. That is, values of permeability should be checked each time a new roll of fabric is introduced.

Sample area variations should have an effect on the coefficient of variation. Larger samples should tend to represent a more average value of permeability, and therefore should have a smaller coefficient of variation. On the other hand, smaller samples should emphasize more fabric irregularities and have a correspondingly higher coefficient of variation. Attempts were made to identify such a trend between the 6.99 cm (2.75 in) diameter air permeability sample area and the 2.54 cm (1 in) diameter falling head sample area, using the data in Appendix C. However, no such trend could be found for any of the fabric types tested. Therefore, at this point, a justified recommendation of sample size on the basis of coefficient of variation cannot be made.

Since the coefficient of variation shows no consistency between fabric types, then the number of samples required to achieve a given accuracy cannot be generally specified. For nonwoven fabrics, the number of samples required to achieve a mean within five percent of the true mean at a 95 percent probability level ranged from 4 to 50. For woven fabrics, the number of required samples ranged from 10 to 69. Therefore, it appears that, for the sample areas used, seven samples per fabric may be arbitrarily chosen as the number of tests to run.

Since the specific falling head test was a newly developed method, it was necessary to consider the variability in results as a function of operator. Table 9 identifies test results obtained for one fabric sample tested by three different operators. The small variation of ten percent probably occurs as a result of timing errors. These could be eliminated through the use of an automatic electric timer, as discussed earlier. However, based on this evidence, it appears that operator variance does not significantly affect the overall test results.

Figure 20 illustrates the effect of fabric thickness on the coefficient of permeability. The change in thickness actually results in a change in gradient since the heads are the same for all thicknesses. The coefficient of permeability increases with increasing thickness (number of layers) until a constant coefficient of permeability is reached at some fabric thickness. It is believed that turbulence is prevalent when fewer layers are tested (i.e. the gradient is higher).

This is to be expected since turbulence depends on the Reynolds number, which depends on the velocity. Velocity, in turn, depends on the hydraulic gradient. For the same heads, the hydraulic gradient decreases as the thickness increases, thereby decreasing the velocity until it is within the laminar range. At this point, the coefficient of permeability assumes a constant value.

Experimentally, the problem of turbulence may be overcome by either of two methods. First, as evidenced by the falling head test results, the number of fabric layers could be increased until the hydraulic gradient was within the laminar range of flow. However, estimation of this thickness will probably vary for different fabric types. Moreover, the falling head test would require modification to eliminate fabric edge leakage that would occur between the permeameter flanges as a result of the increased fabric thickness.

The second alternative to overcome turbulence would be to perform the tests at very low gradients. Giroud [15] estimated this limiting hydraulic gradient of laminar flow to be about one for a needle punched fabric. To achieve very low gradients, a constant head test would be more appropriate. Preliminary test development included the use of a constant head test. The following list identifies the major drawbacks found in this method:

(1) To maintain a constant head, large volumes of water were necessary, due to the high fabric permeabilities. This made deairing difficult, if not impossible.

(2) To avoid any turbulence or jetting effects due to the rapid inflow, care had to be taken to diffuse the flow.

(3) Small heads were very difficult to control accurately.

(4) A constant head test inherently involved an additional measurement - the outflow.

Based on these observations, it was concluded that the constant head test would not represent a quick, simple means of evaluating the fabric coefficient of permeability. Therefore, minimizing the head with this apparatus was not considered as an effective solution. The testing of multiple layers of fabric should be considered the most viable means at present of evaluating k_f in the laminar range.

Figure 19 illustrates the relationship between air and water permittivity measured by the falling head test. Further refinement of this correlation might evolve if truly laminar flow could be accomplished through the use of several layers of fabric. Even at this point, though, it appears that fabric permeability can be confidently predicted with knowledge of the air flow rate. It appears that differences between air and water permittivities are of the same magnitude as the effects of turbulence. The results of the air tests are probably very close to the true laminar flow water values. The final decision as to which method is most suitable (i.e. the air permeability test or the falling head test) must consider the duration and frequency of anticipated testing needs. The air permeability test can be performed more quickly, but initial expenditures are high. On the other hand, initial costs for the falling head permeameter are less, but would be offset by increased labor time during test performance. Therefore, large amounts of testing could be performed more economically with the air permeability equipment.

VII. SUMMARY AND CONCLUSIONS

Fabrics in subdrainage systems perform as either a mechanical support or as a filter for solids suspended in water. In the first instance, the fabric is in intimate contact with the soil. For upward flow, particle migration cannot occur until the soil becomes quick as the seepage force overcomes the weight of the soil and the distributed load from the overburden. An equation was derived to determine the hydraulic gradient responsible for failure attributed to an excessive seepage force with the assumption that arching does not occur after the soil becomes quick. Arching for this case or for downward or horizontal flow will depend on the fabric pore size and the grain size. The stability of these arches requires experimental investigation. If dirty water is being filtered, the fabric is functioning as a filter.

Methods from past research on either granular filters or industrial filtration are suggested as a means of evaluating particle migration and fabric plugging or cake formation. Equations are expressed in terms of fabric permeability, a characteristic soil grain size, and/or the Reynolds number for flow in the soil. An experimental design is proposed to evaluate these suggested relationships, to determine the validity of the theoretical failure gradient for upward flow, and to evaluate the stability of the arches.

The effect of fabric permeability on the line of seepage for a trench drain was evaluated through the use of a hypothetical example. At coefficients of permeability greater than that of the soil, there was virtually no change in the line of seepage with variations in the coefficient.

A falling head test was designed to measure the fabric permeability. The specification of permeability is required to: (1) ensure that water can be removed without the buildup of excessive seepage forces, and (2) minimize particle migration. The final design utilized a 5.08 cm (2 in) diameter cylinder with a 2.54 cm (1 in) diameter orifice. The system was deaired to eliminate inconsistencies attributed to entrapped air.

Air permeability tests were performed for evaluating fabric permeability and for correlation with the falling head test results. Fabric permeabilities were within the range of 10^{-3} to 10^{-1} cm/sec (2×10^{-3} to 2×10^{-1} ft/min) for the fabrics tested with the nonwoven fabrics typically having higher permeabilities than the woven fabrics. Water transmissibility was also expressed in terms of permittivity to minimize fabric bias based on thickness.

The following conclusions have been derived from the above test results and analysis:

(1) Qualitatively, the hydraulic failure gradient for upward flow will depend on the magnitude of the overburden load and the maximum pore size. Arch stability will be a function of the pore size and the grain size.

(2) A fabric coefficient of permeability as low as one tenth the soil permeability will have virtually no effect on the line of seepage.

(3) Fabric permeability can be accurately predicted from air permeability test results.

(4) Turbulence across thin fabrics results in the prediction of a low value of permeability. Without further refinement, the turbulence results in a more conservative estimate of the coefficient of permeability.

(5) Variations between and within fabric lots must be considered in the evaluation of fabric permeability.

VIII. PERMEABILITY TEST RECOMMENDATION

As discussed earlier, the decision to select the air permeability or the water permeability test is strongly dependent upon economics. Either method can satisfactorily predict the coefficient of permeability. The air permeability test has already been developed for other textile applications. This section will focus on recommendations for the performance of a falling head test.

Appendix A describes the test apparatus and procedure. The major features recommended for this test are summarized in the following list:

(1) To provide reasonable time lengths such that they can be recorded with a manual stopwatch, a 5.08 cm (2 in) diameter standpipe with a 2.54 cm (1 in) orifice is recommended. The 30 to 10 cm (11.81 to 3.94 in) water level interval yielded consistent results.

(2) Water and fabric deairing is recommended to eliminate variations due to entrapped air.

(3) Distilled or filtered water should be used to minimize fabric plugging due to water contaminants.

(4) Viscosity corrections should be applied to eliminate variations due to changing water temperatures.

(5) A quick opening mechanism should be employed to ensure free flow during testing.

(6) Samples should be selected that are representative of the lot.

(7) The number of samples required should be determined for different

fabric types and operators such that the mean coefficient of permeability obtained is within five percent of the true mean at a probability level of 95 percent.

(8) The value of k_f calculated under the turbulent conditions may be used for permeability specifications, since it represents a conservative estimate.

IX. RECOMMENDATIONS FOR FUTURE RESEARCH

To fully evaluate filtration mechanisms that might be encountered in subdrainage systems, it is recommended that the following subjects be considered in future research:

(1) The proposed filtration test plan should be executed such that specifications can be more clearly developed.

(2) As mentioned earlier, the number of fabric layers required to ensure laminar flow should be determined experimentally for different fabric types.

(3) The effect of fabric compression or tension on filtration or permeability should be more clearly defined.

(4) Since it is considered desirable to have intimate contact between the fabric and soil, fabric flexibility should be evaluated to determine if the fabric will be able to conform to the shape of any ground irregularities.

(5) The influence of pumping and surging pressures on filtration behavior should be investigated both theoretically and experimentally.

(6) The long-term effects of biological or chemical contaminants on filtration behavior should be investigated through field evaluations.

BIBLIOGRAPHY

1. _____, ASTM Test Procedures, 1977, Annual Book of ASTM Standards, Part 32: Textiles, Yarns, Fabrics, General Test Methods.

2. _____, British Standard Institution, Methods for Textiles, B.S. Handbook No. 11, 1963.

3. _____, "Laboratory Test Report, Polyfilter X (Filter X)," Soil Testing Services, Inc., July 1967.

4. The American Heritage Distionary of the English Language, Davies, P., ed., paperback edition, Dell Publishing Company, Inc., New York, NY, 1973.

5. Ball, John, "Design Parameters for Longitudinal Filter Cloth Lined Subsurface Pavement Drainage Systems," Quarterly Report for the Period January 1, 1978 to March 31, 1978, Submitted to the Alabama State Highway Department, March 31, 1978.

6. Batista, M.J., "Effect of Soil Compaction on Hydraulic Failure of Soils," thesis presented to Utah State University, at Logan, Utah, in 1978, in partial fulfillment of the requirements for the degree of Master of Science.

7. Billings, C.E. and Wilder, J., "Handbook of Fabric Filter Technology," Volume 1, PB-200 648, GCA Corporation, Mass., December 1970.

8. Bourdillon, M., "Utilization of Non-Woven Fabrics for Drainage," (French), Rapport No. 54, Ministere De L-Equipment, Lab. Des Ponts et Chaussees, June 1976, pp. 1-40 (Translated by International Paper Company, Corporate Research Center).

9. Burleigh, E.G., et al., "Pore Size Distribution in Textiles," Textile Research Journal, Volume 19, No. 9, September 1949, pp. 547-555.

10. Calhoun, C.O., "Development of Design Criteria and Acceptance Specifications for Plastic Filter Cloths," Technical Report S-72-7, U.S. Army Corps of Engineers, Waterways Experiment Station, June 1972.

11. Cedergren, H.R., Seepage, Drainage and Flow Nets, 2nd ed., John Wiley and Sons, Inc., New York, NY, 1967.

12. Coates, J. and Pressburg, B.S., "How to Analyze Filtration," Chemical Engineering, Volume 66, No. 20, October 1959, pp. 149-154.

13. Eiland, E. and Lockett, L., "Use of Filter Fabric in French and Trench Subsurface Drains onI-65 in Chilton County, Alabama," presented at the 1976 Annual Meeting of the American Association of State Highway and Transportation Officials at Birmingham, Alabama, November 1976.

14. Letter, H.L. Gyner to J.D. Moreland, "Revision of Edge Drain Detail," Department of Transportation, State of Georgia, May 22, 1978.

15. Giroud, J.P., Personal Communication, Woodward-Clyde Consultants, Chicago, Ill., 1979.

16. Grace, H.P., "Structure and Performance of Filter Media," A.I.Ch.E. Journal, Volume 2, No. 3, September 1956, pp. 307-336.

17. Fulati, O.P., Schwab, G.O. and Reeve, R.C., "Control of Sediment Flow into Subsurface Drains," Journal of the Irrigation and Drainage Division, ASCE, Volume 96, No. IR4, December 1970, pp. 437-449.

18. Hixon, A., Work, L. and Odell, D., TransAmerican Institute of Mineralogy and Metalurgy Engineering, 1926, pp. 73-225.

19. Hoogendoorn, A.D. and Van Der Meulen, J., "Preliminary Investigations on Clogging of Fabrics," Proceedings of the International Converence on the Use of Fabrics in Geotechnics, Ecole Nationale Des Ponts et Chaussees, Volume 2, April 1977, pp. 177-182.

20. Krebs, R.D. and Walker, R.D., Highway Materials, McGraw-Hill Book Company, New York, NY, 1971.

21. Leatherwood, F.N. and Peterson, D.F., "Hydraulic Head Loss at the Interface Between Uniform Sands of Different Sizes," Transactions, American Geophysical Union, Volume 35, No. 4, August 1954, pp. 588-595.

22. List, H.J., "Woven and Non-Woven Fabric Filters in Water Engineering Tests and Dimensioning," (German), Proceedings of International Conference on the Use of Fabrics in Geotechnics, Ecole Nationale Des Ponts et Chaussees, Paris, Volume 2, April 1977, pp. 339-345.

23. Lund, A., "An Experimental Study of Graded Filters," thesis presented to the University of London, in 1949, in partial fulfillment of the requirements for the degree of Master of Science.

24. Mantz, P.E., "Packing and Angle of Repose of Naturally Sedimented Fine Silica Solids Immersed in Natural Aqueous Electrolytes," Sedimentology, Volume 24, No. 6, December 1977, pp. 819-832.

25. Marks, B.D., "The Behavior of Aggregate and Fabric Filters in Subdrainage Applications," Department of Civil Engineering, University of Tennessee, February 1975.

26. Marlar, B.D., "Investigation of Mechanisms Related to Nonwoven Fabric Filtration," thesis presented to the University of Tennessee at Knoxville, Tennessee, in 1975, in partial fulfillment of the requirements for the degree of Master of Science.

27. Mascunana, I., "An Evaluation of PRF-140 Industrial Fabric as Filter Cloth for Underdrains," Illinois Department of Transportation, April 1975.

28. McGown, A., "The Properties and Uses of Permeable Fabric Membranes," Residential Workshop on Materials and Methods for Low Cost Road, Rail, and Reclamation Works, Leura, Australia, September 1976.

29. McGuffey, Verne C., "Filter Fabrics for Highway Construction," Highway Focus, Volume 10, No. 2, May 1978.

30. Muskat, M., "Darcy's Law and the Measurement of the Permeability of Porous Media," The Flow of Homogeneous Fluids Through Porous Media, 1st ed., McGraw-Hill Book Company, Inc., New York, NY, 1937, pp. 55-120.

31. Ogink, H.J.M., "Investigation of the Hydraulic Characteristics of Synthetic Fibers," Delft Hydraulics Laboratory, Publication No. 146, Delft, Holland, May 1975.

32. Ott, L., An Introduction to Statistical Methods and Data Analysis, Guxbury Press, Belmont, California, 1977.

33. Masounave, J., Denis, R., and Rollin, A.L., "Prediction of Hydraulic Properties of Synthetic Non-woven Fabrics Used in Geotechnical Work," submitted for publication to the Canadian Geotechnical Journal, January 1978.

34. Rushton, A., and Griffiths, P.V.R., "Filter Media," Filtration: Principles and Practices, Part 1, Marcel Dekker, Inc., New York, NY, 1977, pp. 252-306.

35. Sweetland, D.B., "The Performance of Nonwoven Fabrics as Drainage Screens in Subdrains," thesis presented to the University of Strathclyde, at Glasgow, Scotland, in 1977, in partial fulfillment of the requirements for the degree of Master of Science.

36. Terzaghi, K. and Peck, R.B., Soil Mechanics in Engineering Practice, 2nd ed., John Wiley and Sons, Inc., New York, NY, 1967.

37. Todd, D.K., "Ground Water Movement," Ground Water Hydrology, John Wiley and Sons, Inc., New York, NY, 1959, pp. 44-77.

38. U.S. Department of the Army, Corps of Engineers, "Plastic Filter Fabric," CW 02215, November 1977.

39. Sample Specifications for Engineering Fabrics, U.S. Department of Transportation, Federal Highway Administration, FHWA-TS-78-211, 1978.

40. U.S. Bureau of Reclamation, "Laboratory Tests on Protective Filters for Hydraulic and Earth Structures," Earth Materials Laboratory, Report #M-132, Denver, Colorado, 1947.

41. Vaughan, P.R., "Design of Filters for the Protection of Cracked Dam Cores Against Internal Erosion," presented at the October 1978 ASCE Convention and Exposition, held at Chicago, Illinois (Preprint 3420).

42. Wakeham, H. and Spicer, N., "Pore Size Distribution in Textiles - A Study of Windproof and Water Resistant Cotton Fabrics," Textile Research Journal, Volume 19, No. 9, September 1949, pp. 703-710.

43. Walker, R.E., "The Interaction of Synthetic Envelope Materials with Soil," thesis presented to Utah State University, at Logan, Utah, in 1978, in partial fulfillment of the requirements for the degree of Master of Science.

44. Cedergren, H.R. and Godfrey, K.A., "Water: Key Cause of Pavement Failure," Civil Engineering, ASCE, Vol. 44, No. 9, Sept., 1974, pp. 78-82.

APPENDICES

APPENDIX A

PROPOSED TEST METHOD FOR WATER PERMEABILITY OF FABRICS

1. Scope

1.1 This method covers the procedure for determining the coefficient of permeability and the permittivity of textile fabrics using the falling head permeameter.

2. Applicable Documents

2.2 ASTM Standards

D 123 Definitions of Terms Relating to Textiles

D 1777 Measuring Thickness of Textile Materials

D 1776 Recommended Practice for Conditioning Textiles and Textile Products for Testing

3. Definitions

3.1 Coefficient of Permeability, n -- the rate of water flow through a material under a differential pressure between the two fabric surfaces expressed in terms of velocity.

3.2 Permittivity, n -- the ratio of the coefficient of permeability to the fabric thickness.

3.3 Permeameter, n -- the equipment used to measure the coefficient of permeability and the permittivity of a fabric.

3.4 For definitions of other textile terms used in this method, refer to Definitions D123.

4. Summary of Method

4.1 The permeameter is filled with distilled, de-aired water. The water is released and the time for the water surface to drop a specified distance is recorded. Knowing the time, temperature and fabric thickness, the coefficient of permeability and permittivity can be determined.

5. Uses and Significance

5.1 The coefficient of permeability is an important factor in the performance of fabrics used in civil engineering applications such as highway drainage, erosion control, and separation between subgrade layers. This property allows for removal of ground water such that excessive seepage forces or hydrostatic pressures do not reduce the stability of the surrounding soil.

5.2 Since information on between-laboratory precision is incomplete, this method is not recommended for acceptance of commercial shipments of fabrics.

6. Apparatus

6.1 Falling Head Permeameter (Figure A-1) consisting of a 6.3 cm (16 in) high, 5.08 cm (2 in) diameter Plexiglass cylinder with a 2.54 cm (1 in) diameter orifice and rubber gaskets to clamp the fabric in place with the aid of six bolts. The base opening is equipped with a rubber stopper and lever for quick release during test performance. The inflow enters through a nozzle near the base. The top of the cylinder is equipped with a nozzle and hose attached to the vacuum source, an opening to vent to the atmosphere, and a thermometer.

6.2 A supply of deaired, distilled water. Filtered tap water may be substituted for distilled water.

6.3 A vacuum pump or aspirator capable of supplying a minimum vacuum of 63.5 cm (25 in) of mercury.

6.4 An electronic stopwatch.

7. Sampling

7.1 Take a lot sample as directed in the applicable material specification. In the absence of such specifications, take a sample comprising ten percent of the rolls in the shipment.

7.2 Take test specimens that are representative of the sample to be tested and free from abnormal distortions.

7.3 Cut specimens to a 6.35 cm (2.5 in) diameter.

8. Number of Specimens and Number of Test Runs

8.1 Unless otherwise agreed upon (as in material specifications), select the number of specimens such that at the 95% probability level, the test result is within 5% of the true mean. Determine the number of specimens as follows:

8.1.1 Reliable Estimate of ν -- When there is a reliable estimate of ν based on past tests of similar materials, calculate the number of specimens using Equation A-1.

$$n = (t^2 \times \nu^2)/A^2 = 0.154 \times \nu^2 \quad \text{(A-1)}$$

where: n = number of specimens (rounded upward to a whole number)

ν = reliable estimate of the coefficient of variation of individual observations on similar materials in the user's laboratory under conditions of single operator precision

t = 1.96, the value of Student's t for infinite degrees of freedom for two-sided limits, and a 95% probability level

A = 5.0% of the average, the value of the allowable variation.

8.1.2 No reliable estimate of ν -- If no estimate of ν is available, test seven specimens. This number of specimens is calculated using ν = 6.7% of the average. When a reliable estimate of ν becomes available, use Equation A-1 to determine the number of specimens.

8.2 For each operator, determine the number of test runs after first running seven timings on one specimen.

8.2.1 Use Equation A-2 to estimate the number of timings required.

$$n_t = (t^2 \times \nu^2)/A^2 = 0.154\ \nu^2 \qquad \text{(A-2)}$$

where: n_t = number of timings (rounded upward to a whole number)

ν = estimate of the coefficient of variation from the seven preliminary timings

t = 1.96, the value of Student's t for infinite degrees of freedom for two-sided limits and a 95% probability level

A = 5.0% of the average, the value of the allowable variation

8.2.2 If n is less than one, obtain two timings.

8.2.3 When a reliable estimate of n becomes available for different time lengths, the operator may assume those values for future runs of the same duration.

9. Conditioning

9.1 Measure thickness as prescribed in Standard Method D 1777 in the standard atmosphere for testing, as described in Recommended Practice D 1776 for each fabric type, with the following exception:

9.1.1 Apply a uniform pressure of 5 g/cm^2 (0.071 psi) over an area of 5 cm^2 (0.78 in^2).

10. Procedure

10.1 Place fabric between flanges. Fasten securely with bolts and wing nuts.

10.2 Ensure that all permeameter external openings are sealed. That is, place stopper in top vent and situate lever over bottom plug.

10.3 Apply a vacuum of 63.5 cm (25 in) of mercury.

10.4 Fill permeameter to the top mark with the vacuum still applied.

10.5 Record the temperature.

10.6 Remove the top rubber stopper to vent the permeameter to the atmosphere.

10.7 Release the bottom lever and plug. Record the time for the water level to fall from the 30 cm (11.81 in) mark to the 10 cm (3.94 in) mark with the stopwatch.

10.8 Repeat Steps 10.2 through 10.7 for additional timings.

10.9 Determine the average test time for each sample.

11. Calculation

11.1 Calculate the coefficient of permeability using Equation A-3.

$$k_f = \frac{a\ L}{At}\ (\ln \frac{h_1}{h_2})\ \frac{u_T}{u_{20}} = 4.3857\ \frac{L\ u_T}{t} \qquad \text{(A-3)}$$

where: k_f = coefficient of permeability

a = area of standpipe

A = cross section area of fabric

L = fabric thickness

h_i = original height of water above fabric

h_f = final height of water above fabric

u_T = viscosity of water at test temperature

u_{20} = viscosity of water at 20°C

t = average test time.

11.2 Calculate the permittivity using Equation A-4.

$$k_p = \frac{k_f}{L} \qquad \text{(A-4)}$$

12. Report

12.1 Report the following items:

12.1.1 Description of the material

12.1.2 Material thickness

12.1.3 Coefficient of permeability

12.1.4 Permittivity

13. Precision and Accuracy

The precision and accuracy of this method is being established.

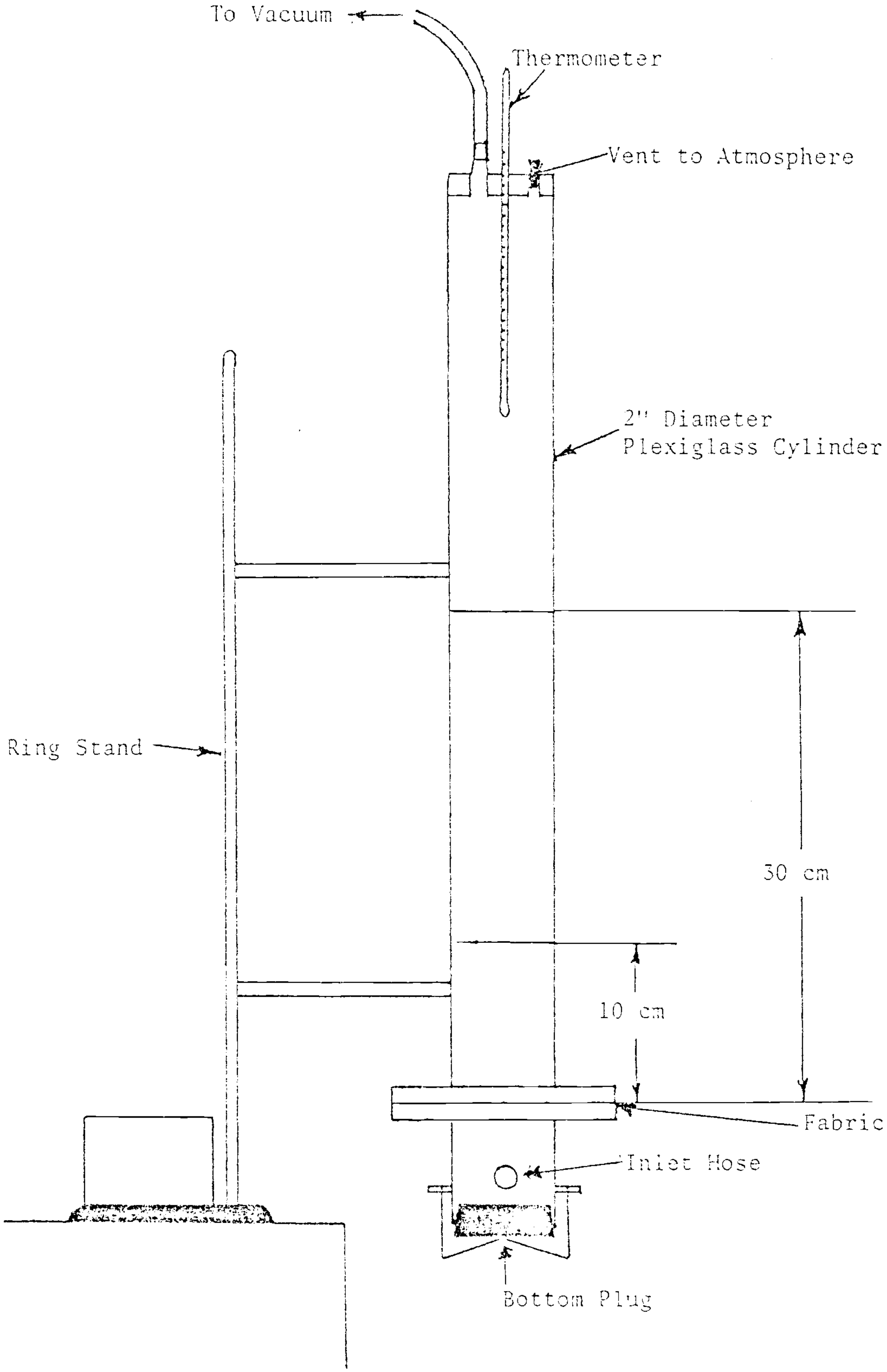

FIGURE A-1. Schematic of Falling Head Test Apparatus

APPENDIX B

SAMPLE CALCULATIONS

Air Permeability Results

To Calculate Permeability, K

$$k = q \frac{\mu L}{\Delta P \ A} \qquad \text{(B-1)}$$

where: q = flow rate, ft^3/min

μ = absolute viscosity of air at room temperature

L = fabric thickness, ft

ΔP = pressure drop across fabric, psf

A = cross sectional area, ft^2

μ: at 21.1°C (70°F) and 65% relative humidity, μ = 183.79 micropoises (Weast, "Handbook of Chemistry and Physics," pg. F-43)

$$1 \text{ dyne} = 2.248 \times 10^{-6} \text{ lb}_f$$

$$1 \text{ poise} = 1 \text{ dyne}\cdot\text{sec/cm}^2$$

$$\mu = 183.79 \times 10^{-6} \text{ dynes}\cdot\text{sec/cm}^2 \times 2.248 \times 10^{-6} \text{ lb/dyne} \times (2.54 \text{ cm/in})^2 \times (12 \text{ in/ft})^2 = 3.838 \times 10^{-7} \text{ lb}\cdot\text{sec/ft}^2$$

ΔP: All fabrics tested at 0.5" water pressure drop across the fabric

$$\Delta P = \frac{\Delta h \text{ inches}}{12 \text{ in/ft}} \times \gamma_w = 0.5/12 \text{ ft} \times 62.314 \text{ pcf} = 2.6 \text{ psf}$$

Note: γ_w at 70°F = 62.314 pcf

A: $A = 1 \text{ ft}^2$ (Values of flow rate specified per one ft^2)

Substituting the values of μ, ΔP, and A into Equation B-1:

$$K = q\ (\mu L/\Delta P\ A)$$

$$K = \frac{3.838 \times 10^{-7}\ \text{lb}\cdot\text{sec/ft}^2 \times 1\ \text{min/60 sec}\ q\ (\text{ft}^3/\text{min})\ L\ \text{ft}}{(2.6\ \text{lb/ft}^2)(1\ \text{ft}^2)}$$

$$K = 2.46 \times 10^{-9}\ q\ L\ \text{ft}^2 \qquad \text{(B-2)}$$

To convert to SI units:

$$K = 2.46 \times 10^{-9}\ \text{ft}^2 \times (30.48\ \text{cm/ft})^2\ q\ L$$

$$= 7.50 \times 10^{-8}\ q\ L\ \text{cm}^2 \qquad \text{(B-3)}$$

q and L in units of ft^3/min and ft, respectively.

<u>To Calculate the Coefficient of Permeability, k_a</u>

$$k_A = \frac{\gamma_{20°C}}{\mu_{20°C}} K \qquad \text{(B-4)}$$

where: $\gamma_{20°C}$ = unit weight of water at 20°C (68°F)

$\mu_{20°C}$ = viscosity of water at 20°C (68°F)

$$k_a = \frac{62.314\ \text{lb/ft}^3}{2.112 \times 10^{-5}\ \text{lb}\cdot\text{s/ft}^2} K = 2.95 \times 10^6\ K\ \text{ft/s} \qquad \text{(B-5)}$$

$$k_a = 8.99 \times 10^5\ K\ \text{cm/sec} \qquad \text{(B-6)}$$

k in units of ft^2.

<u>Statistical Calculations</u>

Standard Deviation: $$s = \sqrt{\frac{1}{n-1}\left[\sum_{i=1}^{n} Y_i^2 - \left(\sum_{i=1}^{n} Y_i\right)^2/n\right]} \qquad \text{(B-7)}$$

where: n = number of samples

y_i = sample value of flow rate

Mean: $$\bar{y} = \frac{\sum_{i=1}^{n} y_i^2}{n} \qquad \text{(B-8)}$$

Coefficient of Variation: $\nu = s/\bar{y} \times 100\%$ (B-9)

Using a Student's t distribution, the number of samples required to obtain a mean within five percent of the true mean at 95 percent probability level is:

$$n_{95} = 0.154\ \nu^2 \qquad \text{(B-10)}$$

At a 90 percent probability level: $n_{90} = 0.108\ \nu^2$ (B-11)

At an 80 percent probability level: $n_{80} = 0.066\ \nu^2$ (B-12)

<u>Example</u>

Given: $q = 458.3\ ft^3/min$

$L = 8.58 \times 10^{-3}\ ft$

Then:

$$K = 2.46 \times 10^{-9}\ q\ L\ ft^2 \qquad \text{(B-2)}$$

$$= (2.46 \times 10^{-9})(458.3)(8.58 \times 10^{-3})$$

$$= 9.7 \times 10^{-9}\ ft^2 = 8.99 \times 10^{-6}\ cm^2$$

and;

$$k_f = 2.95 \times 10^{-6} \times 10^{-6} K = 2.95 \times 10^{6} \times 9.7 \times 10^{-9} \quad (B-5)$$

$$= 2.86 \times 10^{-2} \text{ ft/sec}$$

$$= 8.72 \times 10^{-1} \text{ cm/sec}$$

From previous testing it is known that:

$s = 49.80$

$\bar{y} = 458.29 \text{ ft}^3/\text{min}$

$\nu = 49.80/458.29 \times 100 = 10.87\%$

Therefore:

$$n_{95} = 0.154\ \nu^2 = (0.154)(10.87)^2 = 19 \text{ samples} \quad (B-10)$$

$$n_{90} = 0.108\ \nu^2 = (0.108)(10.87)^2 = 13 \text{ samples} \quad (B-11)$$

$$n_{80} = 0.066\ \nu^2 = (0.066)(10.87)^2 = 8 \text{ samples} \quad (B-12)$$

Water Permeability Results

To Calculate the Coefficient of Permeability at 20°C, k_f

$$k_f = \frac{a\ L}{At} \ln \frac{h_i}{h_f} \frac{\mu_T}{\mu_{20°}}$$

where: a = area of standpipe = π

A = sample area = $\pi(0.5)^2$

h_i = original height of water above fabric sample = 30 cm

h_f = final height of water above fabric sample = 10 cm

t = time for water to fall from h_i to h_f, seconds

μ_T = viscosity of water at test temperature, cp

μ_{20} = viscosity of water at 20°C, cp

L = fabric thickness, cm

$$k_f = \pi/\pi^{\frac{1}{4}} \ln 30/10 \ \mu_T/1.00^2 \ L/t$$

$$= 4.3857 \ L \ \mu_T/t$$

Example

Given: $L = 0.2614$ cm $\mu = 0.7491$

Temp = 33° $t = 1.69$ sec

Then:

$$k_f = (4.3857)(0.2614)(0.7491/1.69)$$

$$= 5.08 \times 10^{-1} \text{ cm/sec}$$

From previous testing it is known that:

$$s = 0.0366$$

$$\bar{y} = 5.27 \times 10^{-1} \text{ cm/sec}$$

$$v = 0.0366/6.27 \times 10^{-1} \times 100 = 6.94\%$$

Therefore:

$$n_{95} = 0.154 \ v^2 = 8 \text{ samples}$$

$$n_{90} = 0.108 \ v^2 = 6 \text{ samples}$$

$$n_{80} = 0.066 \ v^2 = 4 \text{ samples}$$

TABLE B-1. Viscosity of Water

Temperature, °C	Viscosity, cp
20	1.0020
23	0.9325
25	0.8904
26	0.8705
27	0.8513
28	0.8327
29	0.8148
30	0.7975
31	0.7808
32	0.7647
33	0.7491
34	0.7340
35	0.7194
36	0.7052
37	0.6915
38	0.6783
39	0.6654
40	0.6529

From: Handbook of Chemistry and Physics," R.C. Weast, ed., 51st ed., The Chemical Rubber Company, 1970, F36.

APPENDIX C

TEST RESULTS

TABLE C-1. Summary of Air Permeability Test Results

Fabric Number	Number of Samples	Flow Rate $ft^3/min/ft^2$ Maximum	Minimum	Mean, $\bar{y}$	Standard Deviation	Coefficient of Variation %	Number of Samples Required n_{95}	n_{90}	n_{80}
NONWOVEN									
NW-1 (3)	7	385	340	357.4	18.0	5.0	4	3	2
NW-2 (4)	7	340	256	300.5	30.9	10.3	17	12	7
NW-3 (4)	7	102.5	63.5	79.0	12.5	15.8	39	27	17
NW-4 (8)	7	315	277.5	295.7	12.9	4.4	3	3	2
NW-5 (17)	7	208.5	136	175.8	23.1	13.1	27	19	12
WOVEN									
W-1 (4)	7	7.7	6.4	7.2	0.5	6.9	8	6	4
W-2 (7)	7	169	124	142.8	17.0	11.9	22	16	10
W-3 (8)	7	11.6	7.2	9.6	1.3	13.4	28	20	12
COMBINATION									
C-1 (4)	7	33.8	23.5	27.1	3.6	13.4	28	20	12

Note: $1\ cm^3/cm^2 \cdot sec = 1.969\ ft^3/ft^2 \cdot min.$